GEOLOGIC BACKGROUND AND MAP UNIT DESCRIPTIONS TO ACCOMPANY BEDROCK GEOLOGIC MAPS OF THE WESTERN TANACROSS AND TAYLOR MOUNTAIN AREAS, TANACROSS AND EAGLE QUADRANGLES, ALASKA

Travis J. Naibert, Alicja Wypych, Rainer J. Newberry, Evan Twelker, Michelle M. Gavel, Alec D. Wildland, Michael L. Barrera, David J. Szumigala, Sean P. Regan, Dylan F. Avirett, Curtis M. Bernard, Noel J.S. Blackwell, Serena N. Fessenden, David A. Harvey, Angie K. Hubbard, Steve S. Masterman, Izzy P. Muller, Mark M. Turner, and W. Chris Wyatt

Preliminary Interpretive Report 2024-6A

2024
STATE OF ALASKA
DEPARTMENT OF NATURAL RESOURCES
DIVISION OF GEOLOGICAL & GEOPHYSICAL SURVEYS

STATE OF ALASKA
Mike Dunleavy, Governor

DEPARTMENT OF NATURAL RESOURCES
John Boyle, Commissioner

DIVISION OF GEOLOGICAL & GEOPHYSICAL SURVEYS
Melanie Werdon, State Geologist & Director

Publications produced by the Division of Geological & Geophysical Surveys are available to download from the DGGS website (dggs.alaska.gov). Publications on hard-copy or digital media can be examined or purchased in the Fairbanks office:

Alaska Division of Geological & Geophysical Surveys (DGGS)
3354 College Road | Fairbanks, Alaska 99709-3707
Phone: 907.451.5010 | Fax 907.451.5050
dggspubs@alaska.gov | dggs.alaska.gov

DGGS publications are also available at:

Alaska State Library, Historical
Collections & Talking Book Center
395 Whittier Street
Juneau, Alaska 99801

Alaska Resource Library and
Information Services (ARLIS)
3150 C Street, Suite 100
Anchorage, Alaska 99503

Suggested citation:
Naibert, T.J., Wypych, Alicja, Newberry, R.J., Twelker, Evan, Gavel, M.M., Wildland, A.D., Barrera, M.L., Szumigala, D.J., Regan, S.P., Avirett, D.F., Bernard, C.M., Blackwell, N.J., Fessenden, S.N., Harvey, D.A., Hubbard, A.K., Masterman, S.S., Muller, I.P., Turner, M.M., and Wyatt, W.C., 2024, Geologic background and map unit descriptions to accompany bedrock geologic maps of the western Tanacross and Taylor Mountain areas, Tanacross and Eagle quadrangles, Alaska, *in* Naibert, T.J., ed., Geologic investigation of the Western Tanacross and Taylor Mountain areas, Tanacross and Eagle quadrangles, Alaska: Alaska Division of Geological & Geophysical Surveys Preliminary Interpretive Report 2024-6A, 39 p. https://doi.org/10.14509/31167

Contents

Figures

Tables

GEOLOGIC BACKGROUND AND MAP UNIT DESCRIPTIONS TO ACCOMPANY BEDROCK GEOLOGIC MAPS OF THE WESTERN TANACROSS AND TAYLOR MOUNTAIN AREAS, TANACROSS AND EAGLE QUADRANGLES, ALASKA

Travis J. Naibert[1], Alicja Wypych[1], Rainer J. Newberry[1], Evan Twelker[1], Michelle M. Gavel[1], Alec D. Wildland[1], Michael L. Barrera[1], David J. Szumigala[1], Sean P. Regan[2], Dylan F. Avirett[1], Curtis M. Bernard[2], Noel J.S. Blackwell[1], Serena N. Fessenden[1], David A. Harvey[1], Angie K. Hubbard[1], Steve S. Masterman[1], Izzy P. Muller[1], Mark M. Turner[1], and W. Chris Wyatt[1]

INTRODUCTION

The Alaska Division of Geological & Geophysical Surveys (DGGS) Mineral Resources section conducted bedrock geological mapping of a 4,450-sq-km (1,720-sq-mi) area in eastern Interior Alaska around Mosquito Flats, herein called the Western Tanacross project, and a 2,320-sq-km (900-sq-mi) area around Taylor Mountain and the Mosquito Fork of the Fortymile River, herein called the Taylor Mountain project (fig. 1). The Western Tanacross project area straddles the Alaska Highway northwest of Tok, Alaska and includes most of the Tanacross Quadrangle not previously mapped by DGGS (Sicard and others, 2017; Wypych and others, 2021; Twelker and others, 2021; Werdon and others, 2019). The Taylor Mountain project lies south and west of Chicken, Alaska and straddles the Taylor Highway northeast of Tok, Alaska. The project includes a portion of the northern Tanacross Quadrangle as well as the parts of the southern Eagle Quadrangle. DGGS and the U.S. Geological Survey (USGS) identified these map areas as having potential to host deposits of multiple critical minerals (Hammarstrom and Dicken, 2019; Kreiner and Jones, 2020; Kreiner and others, 2022), as well as conventional mineral resources including gold, copper, molybdenum, lead, zinc, and silver. Most of the known mineralization in both project areas is related to Mesozoic-Paleogene magmatism, which includes diverse compositions, emplacement depths, and varying intrusion sizes. Igneous rocks intrude a composite metamorphic province that includes both parautochthonous North America and the allochthonous Yukon Tanana Terrane, which are both multiply deformed and apparently juxtaposed along low-angle faults.

The Western Tanacross and Taylor Mountain maps and associated geologic reports are a product of 460 person-days of helicopter-supported fieldwork completed during the summers of 2021 and 2022, plus compilation and reinterpretation of existing geologic maps (Foster, 1967; Foster, 1970; Foster, 1976). Age assignments for igneous and metaigneous map units are supported by 38 new U-Pb zircon ages completed as part of this study (Gavel and others, 2023). Cooling ages of metamorphic rocks, hydrothermal alteration ages, and crystallization ages for select igneous rocks are informed by 22 new $^{40}Ar/^{39}Ar$ ages (Naibert and others, 2023). Seven detrital zircon analyses were conducted to better understand Cretaceous sedimentary rocks and Paleozoic-Proterozoic metasedimentary rocks in the study area (Gavel and others, 2023). All cited age uncertainties are reported at 2σ, and uncertainties have been converted from their original sources to 2σ where applicable. We used geochemical data, including 388 whole-rock analyses (Wypych and others, 2022a, 2022b), more than 300 slab X-ray fluorescence (XRF) analyses, and more than 2,500 handheld XRF analyses, to describe, classify, and map the distribution of different lithologies in both map areas. In addition to our own data, this map is built on open exchange of data and ideas with our colleagues at the USGS Alaska Science Center.

[1] Alaska Division of Geological & Geophysical Surveys, 3354 College Road, Fairbanks, Alaska 99709
[2] Geophysical Institute, University of Alaska Fairbanks, 900 Yukon Drive, Fairbanks, AK 99775

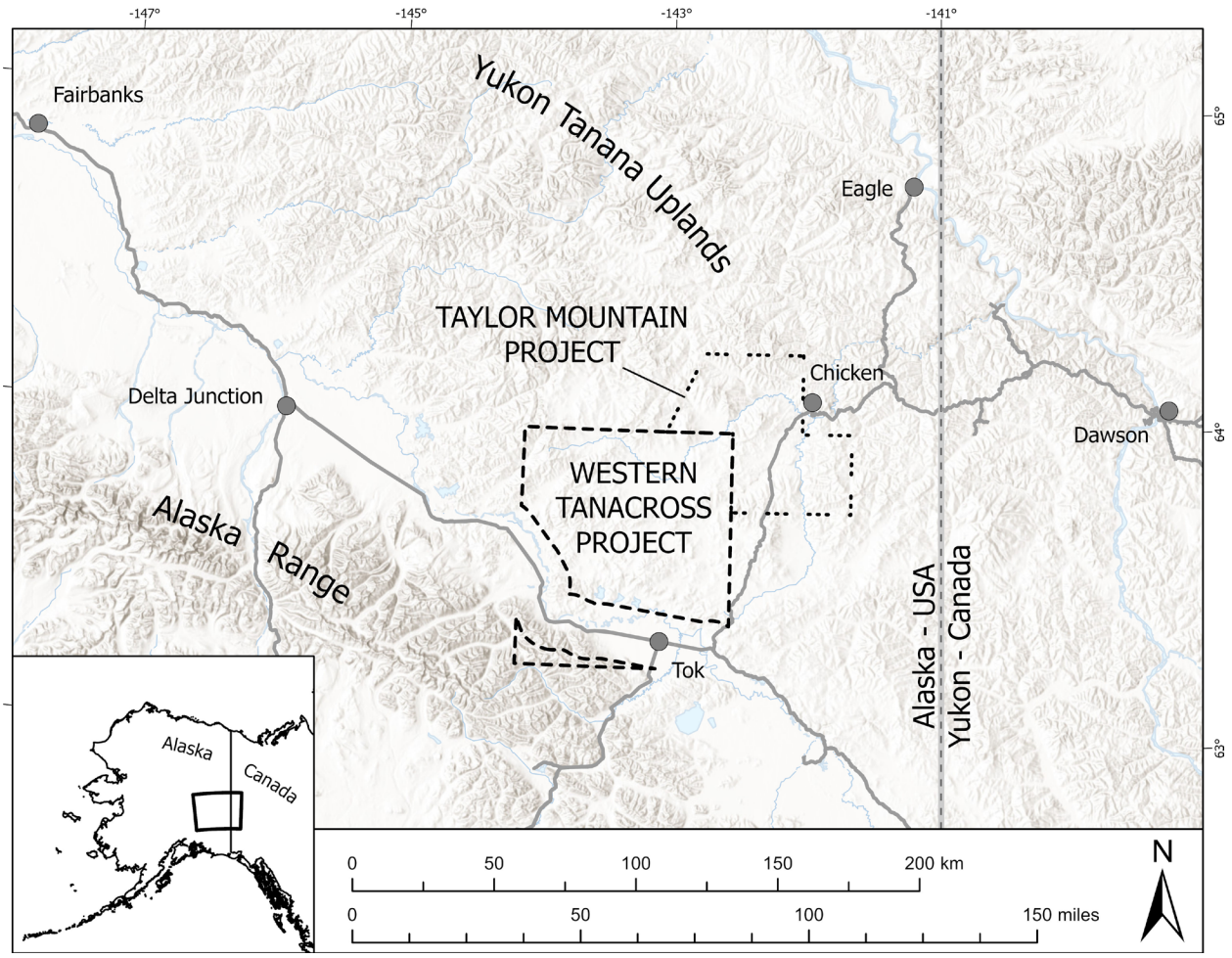

Figure 1. Map showing the location of the Western Tanacross and Taylor Mountain project areas.

Both map areas lie in the Yukon-Tanana Upland, which is characterized by moderate-relief, thickly vegetated hills. Evidence for Pleistocene glaciation was identified by Weber and Wilson (2012) at high elevations on Taylor Mountain, Kechumstuk Mountain, and Diamond Mountain, but is not part of this study. Eolian deposits in the area are generally thin. Outcrops are minimal in valleys and on vegetated hillsides and sparse along lower elevation ridgelines. Small parts of both map areas include ridges above treeline and more continuous rock exposure is observed along these ridges, but intact outcrops are still discontinuous. The southwest part of the Western Tanacross project includes part of the eastern Alaska Range south of the Alaska Highway. Higher elevations and significant relief in this part of the map area result in more extensive outcrop exposure. Our map interpretation relies on rock descriptions of outcrop, subcrop, and float samples, and we have made extensive use of airborne geophysical surveys (Burns and others, 2015, 2019; Emond and others, 2015; Emond and MPX, 2021) for interpolation between field stations.

REGIONAL GEOLOGY

The Western Tanacross and Taylor Mountain project areas both comprise two terranes: the allochthonous Yukon Tanana Terrane (YTT) and the parautochthonous North American margin (pNA). The oldest rocks in the YTT include pre-Mississippian metasedimentary and metaigneous rocks interpreted to have rifted from the western margin of North America (Laurentia) during the Late Devonian-Early Mississippian

(Dusel-Bacon and others, 2006). A series of Paleozoic to early Mesozoic volcanic arcs and related intrusions are built on the pre-Mississippian rocks. The arc rocks and coeval sediments of the YTT share a metamorphic and tectonic history that is distinct from the autochthonous North American margin. The YTT was accreted to North America during the Mesozoic (Dusel-Bacon and others, 2002; Dusel-Bacon and others, 2015). Collision of the YTT and pNA was complete prior to extensive mid-Cretaceous magmatism that affected both terranes. Exhumation of pNA from beneath YTT occurred along low-angle extensional shear zones and is recorded by mid-Cretaceous cooling ages of metamorphic rocks throughout the region (Hansen and others, 1991; Pavlis and others, 1993; Hansen and Dusel-Bacon, 1998; Dusel-Bacon and others, 2002). Internal imbrication within YTT, Mesozoic collision with pNA, and later extension resulted in a structurally complex boundary between YTT and pNA. Magmatism continued into the Paleogene, with discrete periods of mid-Cretaceous, Late Cretaceous, and early Paleogene volcanism and plutonism across the Yukon-Tanana Uplands and adjacent Western Yukon (Bacon and others, 1990, 2014; Twelker and others, 2021; Wypych and others, 2021). Quaternary volcanism was recognized in the adjacent Northeast Tanacross area (Mertie, 1931; Blondes and others, 2007; Wypych and others, 2021). Multiple sets of high-angle faults developed after mid-Cretaceous ductile extension and exhumation of pNA. These faults are variably mapped with both strike-slip and dip-slip motion, based on apparent offset of pluton contacts and cross-cutting relationships with older structures.

Parautochthonous North America

Rocks of pNA in the project areas include the Lake George assemblage and Jarvis assemblage (named the Jarvis belt by Dashevsky and others [2003]), which are interpreted to be the higher-grade equivalents of Paleozoic to Neoproterozoic marginal basin strata exposed in the Selwyn basin northeast of the Tintina fault (Mair and others, 2006; Dusel-Bacon and others, 2006; Murphy and others, 2009). These sedimentary rocks were intruded by Devonian-Early Mississippian intrusions, which were metamorphosed to orthogneiss, and by Cretaceous and Paleogene intrusions following Early Cretaceous peak-metamorphism (Wildland, 2022). Evidence of Late Mississippian to Jurassic periods of magmatism that are found in the YTT are notably absent in pNA. Metamorphic rocks of the Lake George and Jarvis assemblages in eastern Alaska have characteristic sub-horizontal foliations that are at least second-generation, which are recognized at many locations as an axial-planer foliation related to isoclinal folding of an older foliation. Parautochthonous rocks have mid-Cretaceous $^{40}Ar/^{39}Ar$ cooling ages, suggesting exhumation from above 300–500°C between ca. 125–105 Ma (Dusel-Bacon and others, 2002; Naibert and others, 2020, Jones and Benowitz, 2020).

The Lake George assemblage includes most of the pNA rocks exposed in the Yukon Tanana Uplands between the Yukon-Alaska border and the Salcha River area, as well as along the northern edge of the eastern Alaska Range (Dusel-Bacon and others, 2006). The Lake George assemblage protoliths are quartzose and pelitic sediments with Precambrian detrital zircon (Gavel and others, 2023), which were intruded in the Late Devonian to Early Mississippian by felsic to mafic intrusions prior to being metamorphosed. The Lake George assemblage is composed of quartzite, paragneiss, quartz schist, amphibolite, and granitic to dioritic composition orthogneiss. Orthogneiss boundaries within the Lake George assemblage are not often exposed but are generally concordant with foliation, indicating either original layer-parallel intrusive contacts or transposition of intrusive contacts into foliation during deformation. Orthogneiss layers are decimeters to hundreds of meters thick (Wypych and others, 2021). In western Yukon, the Scottie Creek Formation and the Mount Baker intrusive suite may correlate to metasedimentary and metaplutonic subunits of the Lake George assemblage, respectively (Ryan and others, 2014). Dusel-Bacon and others

(2006) suggested the Lake George assemblage shares similar protoliths and depositional settings with the Fairbanks–Chena assemblage, though that assemblage is more quartz-rich and does not include as many metaplutonic rocks. Those authors correlate the Fairbanks–Chena assemblage to the Hyland Group in the Selwyn Basin in Yukon and that correlation may apply to parts of the Lake George assemblage as well.

The Divide Mountain suite is composed of megacrystic granitoid plutons intruded into the Lake George assemblage in the Early Mississippian and metamorphosed to amphibolite facies, resulting in distinctive alkali feldspar augen gneiss bodies throughout the region (Twelker and others, 2021, Wypych and others, 2021). Both foliation concordant and discordant contacts were observed between Divide Mountain augen gneiss and Lake George assemblage subunits. Discordant contacts may be original intrusive contacts that cross-cut lithologic layering. U-Pb zircon ages of augen gneiss in eastern Alaska are ca. 371 to 347 Ma (Dusel-Bacon and others, 2006; Todd and others, 2019; Jones and O'Sullivan, 2020; Wildland and others, 2021). Deformation fabrics in the Divide Mountain augen gneiss are varied. Some exposures are weakly foliated and alkali feldspar porphyroclasts are euhedral. Other exposures are strongly foliated and porphyroclasts have been rotated or stretched along foliation planes and often are surrounded by mineral tails forming sigma or delta clasts.

The Jarvis assemblage is exposed in the eastern Alaska Range in the southwest corner of the Western Tanacross map area extending south into the Tok River area (Sicard and others, 2017) and the Delta mineral belt (Dashevsky and others, 2003). The Jarvis assemblage is also exposed along the north side of the Alaska Highway southeast of Tetlin Junction (Solie and others, 2019; Twelker and others, 2021). The Jarvis assemblage has been correlated with the White River assemblage in adjacent areas in western Yukon (Murphy and others, 2009; Twelker and others, 2021; Ryan and others, 2014). Quartzose sediments and subordinate pelitic and calcareous sediments, which are interlayered with minor Late Devonian to Mississippian felsic volcanic and volcaniclastic rocks, dominate the structurally lowest parts of the Jarvis assemblage. Volcanic and volcaniclastic protoliths become increasingly abundant up section to the south in the Tok River area (Sicard and others, 2017). The Jarvis assemblage was metamorphosed to lower amphibolite facies, a history that is variably overprinted by retrograde greenschist facies metamorphism north of the Tanana River and in the Alaska Range (Newberry and Twelker, 2021). U-Pb zircon ages from metaigneous layers are Mississippian to Devonian and are interpreted to record an active volcanic arc at that time (Dashevsky and others, 2003). The Jarvis assemblage is separated from the underlying Lake George assemblage by a low- to moderate-angle fault contact. The Jarvis assemblage is intruded by metamorphosed gabbro sills, which have yielded multiple Triassic ages (Gavel and others, 2023; Sicard and others, 2017). These sills are not observed in the underlying Lake George assemblage. Similar sills, called the Snag Creek gabbros, are observed in the correlative White River assemblage in Yukon (Murphy and others, 2009; Ryan and others, 2014). Triassic gabbro of the Galena suite intrudes the Earn and Tsichu groups in the Selwyn Basin (Skipton, 2022) and have similar Triassic ages and geochemistry to gabbro in the Jarvis assemblage (Colpron and others, 2023). These similarities suggest that the Jarvis assemblage is the more-metamorphosed equivalent of the Devonian-Mississippian Earn Group and Mississippian Tsichu Groups of the Selwyn Basin.

Yukon Tanana Terrane

Rocks of YTT in the map areas include the Fortymile River assemblage and Chicken assemblage. Other YTT assemblages in the region include the Finlayson, Snowcap, Nasina, Klondike, and Ladue River assemblages. The YTT is interpreted as a multiply-deformed, pericratonic continental fragment that rifted away from western North America, likely from present-day northern British Columbia and Alaska,

starting in the Late Devonian (Nelson and others, 2006). Early Mississippian Finlayson arc, Late Mississippian-Pennsylvanian Klinkit arc, and Late Permian Klondike arc magmatism affected parts of the YTT prior to accretion to North America in the Triassic to Early Jurassic (Colpron and others, 2006). Most YTT rocks have Latest Triassic to Early Jurassic $^{40}Ar/^{39}Ar$ cooling ages, suggesting exhumation from above 300–500°C at those times (Hansen and others, 1991; Dusel-Bacon and others, 2002; Naibert and others, 2020, Jones and Benowitz, 2020). These cooling ages have been interpreted to record thrusting of the YTT onto rocks of the North American margin (Hansen and Dusel-Bacon, 1998; Dusel-Bacon and others, 2015). Many cooling ages in the Ladue River assemblage and some cooling ages in adjacent parts of the Klondike assemblage are Permian to Triassic, indicating that those assemblages had already exhumed prior to Early Jurassic collision and may have been structurally higher levels of the YTT during final accretion (Jones and Benowitz, 2020; Naibert and others, 2020).

The Fortymile River assemblage is the most widely exposed YTT assemblage in eastern Alaska and is correlated with the Finlayson assemblage in Yukon. Pre-Mississippian metasediments in the Fortymile River assemblage, which may correlate with the Snowcap assemblage, are similar to continental margin rocks of North America, supporting the interpretation that YTT is a rifted continental fragment of North America (Nelson and others, 2006). The Fortymile River and Finlayson assemblages are composed of Upper Devonian to Lower Mississippian bimodal metaigneous rocks representing both arc and back-arc magmatism following rifting (Colpron and others, 2006). These arc rocks are called the Finlayson arc by Colpron and others (2006). The metaigneous rocks in the Fortymile River assemblage are interlayered with paragneiss, quartz schist, locally thick marble layers, and abundant amphibolite. Coeval arc plutons (Simpson Range suite in Yukon) as well as Devonian to Early Mississippian rift-related within-plate plutons (Grass Lakes suite in Yukon) intrude lower levels of the Fortymile River and Finlayson assemblages and the underlying Snowcap assemblage (Piercey and others, 2006). The Snowcap assemblage in Yukon is also intruded by large Late Permian intrusions of the Sulphur Creek suite (Ryan and others, 2014), which are interpreted to be the roots of the Permian Klondike arc. Small amounts of Permian orthogneiss have been documented in the Fortymile River assemblage in eastern Alaska (Jones and others, 2017). The Fortymile River assemblage is also intruded by both Late Triassic and Early Jurassic plutons, which are largely unmetamorphosed and undeformed, indicating that peak metamorphic conditions were pre-Jurassic.

The Chicken assemblage, previously mapped as the Chicken Metamorphic Complex by Werdon and others (2001), is exposed in the Taylor Mountain map area and in the southwest corner of the Eagle A-2 Quadrangle. The Chicken assemblage is dominated by fine- to coarse-grained mafic to intermediate metaigneous rocks with arc geochemistry and minor metasedimentary rocks including fine-grained quartzite, meta-arkosic sandstone, and locally thick but discontinuous marble layers. These rocks have been metamorphosed to greenschist facies and are minimally deformed with primary igneous textures commonly observed. This lack of pervasive deformation contrasts with the moderately to strongly foliated metamorphic units in other Yukon-Tanana Terrane assemblages. We interpret fine-grained greenstones within the Chicken assemblage as volcanic flows or tuff, as they are interlayered with metasediments. We interpret coarser-grained metagabbros as dikes and sills. Gabbro in the Chicken assemblage is Middle Mississippian (ca. 347 to 339 Ma; Gavel and others, 2023; Jones and O'Sullivan, 2020). A detrital zircon sample from quartzite yielded a maximum depositional age of 355 Ma. The detrital zircon sample also yielded Precambrian grains indicating sediment recycling from either the Fortymile River assemblage or the North American margin (Gavel and others, 2023). The Chicken assemblage is intruded by multiple Late Triassic

intrusions, including the Taylor Mountain Batholith. Both outcrop observations and microprobe analysis of plagioclase and amphibole suggest hornblende-hornfels facies contact metamorphism is common in the Chicken assemblage, which was likely caused by these Triassic intrusions. Two Late Triassic $^{40}Ar/^{39}Ar$ ages from greenstones (Werdon and others, 2001) likely record hornblende age reset due to these intrusions. The Chicken assemblage has previously been correlated with the Seventymile assemblage of the Slide Mountain terrane (Foster and others, 1994), but the lack of ultramafic rocks characteristic of the Slide Mountain terrane and the arc geochemistry of the mafic volcanic rocks do not support this correlation. We suggest the Chicken assemblage is correlative with rocks of the Klinkit arc, most likely the mafic volcanic and volcaniclastic rocks in the Butsih Formation of the Klinkit Group (Simard and others, 2003) in northern British Columbia. Other possible correlations include another part of the Klinkit arc, the Little Salmon Formation in southern Yukon (Colpron, 2001), or Paleozoic basement to Quesnellia such as the Moose Formation of the Boswell assemblage (Moynihan and Crowley, 2022), also in Yukon.

The Nasina assemblage is exposed north of the Taylor Mountain map area in the Eagle Quadrangle and extends into adjacent parts of Yukon. The Nasina assemblage consists of variably carbonaceous quartzite, phyllite, schist, marble, and minor greenstone, metatuff, and stretched pebble conglomerate (Dusel-Bacon and others, 2006), which are interpreted to have been deposited in a back-arc basin setting. Most of the Nasina assemblage experienced greenschist facies metamorphism, though some garnet and sillimanite indicate amphibolite facies conditions were reached in some locations in Yukon (Beranek and Mortensen, 2011). Concordant felsic layers have both Devonian-Mississippian and Late Permian ages, suggesting either a long-lived basin, an unrecognized unconformity, or that some of the felsic layers are sills or transposed dikes (Dusel-Bacon and others, 2006). The Nasina assemblage is mapped in the footwall beneath a thrust panel of Fortymile River assemblage in the Eagle Quadrangle (Foster, 1976; Dusel-Bacon and others, 2006), but was not mapped in the Taylor Mountain or Western Tanacross project areas.

The Ladue River assemblage is exposed southeast of the map areas around the Ladue River on the Alaska side of the Yukon border. The assemblage was initially defined as the Ladue River Unit by Dusel-Bacon and others (2006) and was originally mapped by Foster (1970) as a greenschist-facies unit possibly correlated with the Permian Klondike assemblage, but was later found to contain Late Devonian metaigneous rocks (Dusel-Bacon and others, 2006). Protoliths in the Ladue River assemblage are very similar to the Fortymile River assemblage, including paragneiss, orthogneiss, and schist, but the Ladue River assemblage lacks the Jurassic and Triassic plutons that are intruded into the Fortymile River assemblage. Most $^{40}Ar/^{39}Ar$ cooling ages in the Ladue River assemblage are Permian to Triassic instead of Early Jurassic, as is common in the Fortymile River assemblage (Jones and Benowitz, 2020). The Ladue River assemblage was not mapped in the Taylor Mountain or Western Tanacross project areas and further description can be found in Twelker and others (2021).

The Klondike assemblage is exposed east of the map areas in eastern Alaska and western Yukon and consists of Middle to Late Permian metavolcanic rocks of the Klondike arc (Colpron and others, 2006) and interbedded metasediments metamorphosed to greenschist facies (Twelker and others, 2021). Metavolcanic rocks are dominantly felsic in Yukon (Ryan and others, 2014), but include significant mafic layers in Alaska (Twelker and others, 2021). The Klondike assemblage is intruded by coeval plutons of the Sulphur Creek suite, which also intrude the Snowcap and Finlayson assemblages in Yukon. The Klondike assemblage was mapped to the east of the Western Tanacross project area by Twelker and others (2021).

Seventymile/Slide Mountain Terrane

The Seventymile terrane in eastern Alaska, and the equivalent Slide Mountain terrane in Yukon and British Columbia consist of fault-bound slices of serpentinized ultramafic rocks, weakly metamorphosed mafic rocks, and Mississippian to Upper Triassic marine sediments (Dusel-Bacon and others, 2006; Colpron and others, 2006). The Seventymile terrane is generally interpreted as a dismembered ophiolite sequence that marks major thrust faults between the YTT and pNA (Dusel-Bacon and others, 2006; Nelson and others, 2006).

Post-Metamorphic Magmatism

Multiple discrete pulses of magmatism affected the Yukon Tanana Uplands region between the Permian and the Quaternary. The little-deformed pluton on the summit of Mount Warbelow in the Eagle A-3 Quadrangle has yielded Permian ages (Gavel and others, 2023; Jones and others, 2017). The pluton intrudes the Fortymile River assemblage. Late Triassic magmatism of the Taylor Mountain plutonic suite includes the Taylor Mountain Batholith, Diamond Mountain pluton, Kechumstuk pluton, and related dikes/sills and smaller intrusions (Werdon and others, 2001; Day and others, 2014; Wypych and others, 2021). The Taylor Mountain suite primarily intruded the Chicken assemblage, but also intruded the Fortymile River assemblage on the south side of Taylor Mountain. Jurassic magmatism of the herein-named Napoleon Creek suite includes plutons and related dikes in the Eagle A-1 and A-2 quadrangles (Werdon and others, 2001; Szumigala and others, 2002b), multiple intrusions on the north and west sides of Mosquito Flats, the Mount Veta intrusion (Day and others, 2014), and similar dikes/stocks in the Taylor Mountain area. The Napoleon Creek suite intrudes both the Chicken assemblage and Fortymile River assemblage and were emplaced during exhumation of the Fortymile River assemblage in the Early Jurassic. The Triassic to Jurassic magma pulses were caused by east-dipping subduction following the initial collision of YTT with pNA (Dusel-Bacon and others, 2015) but prior to final thrusting of YTT rocks over pNA margin, since the pNA rocks lack pre-Cretaceous intrusions.

We define the mid-Cretaceous Mount Harper (ca. 104–114 Ma) and Gardiner Creek (ca. 95–104 Ma) plutonic suites in eastern Alaska, which intrude both pNA and YTT rocks. Intrusion of the Mount Harper plutonic suite, named for the Mount Harper Batholith in the Eagle Quadrangle, was syn- to post-exhumation of pNA during regional extension. Batholith-scale plutons are intruded into the Lake George assemblage and intrusions in the overlying YTT are often smaller stocks or dikes. The Mount Harper suite is dominantly biotite-bearing granite, lesser two-mica and garnet-bearing peraluminous granite, and minor granodiorite. Volcanic rocks of overlapping age are mapped at Sixtymile Butte and near the West Fork of the Dennison Fork River (Bacon and others, 1990). The younger Gardiner Creek plutonic suite intrudes the Lake George assemblage, the Jarvis assemblage, and the Ladue River assemblage. It is dominantly biotite- and hornblende-bearing granodiorite, though both plutonic suites vary from granite to gabbro.

Magmatism resumed in the Late Cretaceous with porphyry intrusions of the Taurus suite at the Taurus and Pika prospects in the northeast Tanacross Quadrangle (Wypych and others, 2021) and similar rocks at the Casino deposit in Yukon, which host copper-molybdenum-gold mineralization (Allen and others, 2013). Alkaline intrusions of the Mount Fairplay suite were also intruded in the Late Cretaceous (Foster 1967; Twelker and others, 2021). Volcanic rocks of the Carmacks Group in Yukon and eastern Alaska, as well as the Middle Fork Caldera (Bacon and others, 1990) were erupted along NE-striking faults. Volcanics and shallow intrusions mapped along the Sixtymile–Pika fault zone by Wypych and others (2021) also suggest fault-related magma ascent and local basin development during this time.

A scattered pulse of Paleocene to Eocene (ca. 60–55 Ma) magmatism resulted in both felsic and mafic dikes and small plugs as well as scattered rhyolite tuffs throughout eastern Alaska (Twelker and others, 2021; Werdon and others, 2001). This magmatism was more extensive in western Yukon in the Rhyolite Creek complex and the Ruby Range plutonic suite (Allan and others, 2013). Quaternary basanite at Prindle Volcano is the youngest magmatism in the region (Wypych and others, 2021).

Mesozoic to Cenozoic Faulting

Assemblages in the YTT were internally deformed and exhumed prior to the Middle Jurassic and possibly as early as the Late Permian, as evidenced by Permian to Triassic $^{40}Ar/^{39}Ar$ cooling ages in the lower-amphibolite-facies Ladue River assemblage and metamorphic xenoliths observed in the Mount Warbelow pluton (Jones and others, 2017). Internal thrust imbrication likely caused cooling in the Fortymile River assemblage in the Early Jurassic as it was thrust over greenschist-facies Chicken assemblage, Klondike assemblage, and Nasina assemblage rocks in the Eagle Quadrangle (Foster, 1976; Dusel-Bacon and others, 2006). In western Yukon, YTT assemblage thrust stacking appears complicated, with multiple mapped thrusts placing both amphibolite-facies assemblages over greenschist-facies assemblages, and greenschist-facies assemblages over amphibolite-facies assemblages (Yukon Geological Survey, 2019). Contraction in the latest Triassic to Early Jurassic likely resulted in initial thrusting of YTT over the distal edges of the North American margin, though the lack of Triassic-Jurassic intrusions in currently exposed parts of pNA suggest that final thrusting of YTT onto the North American margin occurred after the Early Jurassic. Thrust faults as old as the Late Permian are mapped within the YTT and between the YTT, Seventymile/Slide Mountain terrane, and North America in the Finlayson Lake area in Yukon (Murphy and others, 2006). Early Jurassic extension has also been documented along the Willow Lake Fault in Yukon (Knight and others, 2013), which is interpreted to have occurred either synchronous with or immediately following Jurassic thrust faulting in YTT. It is unclear how widespread syn-orogenic extension was in the region during the Jurassic.

A low-angle extensional detachment and accompanying zone of hanging wall shear is poorly exposed between the Fortymile River assemblage and the Lake George assemblage in the northeastern Tanacross Quadrangle (Hansen and Dusel-Bacon, 1998; Wypych and others, 2021). Mid-Cretaceous $^{40}Ar/^{39}Ar$ cooling ages in the footwall and adjacent parts of the hanging wall suggest exhumation during extension in the mid-Cretaceous (Dusel-Bacon and others, 2002; Naibert and others, 2020). Hansen and Dusel-Bacon (1998) document top-to-the-southeast shear along the detachment and throughout the footwall. Sections of low-angle faults separating the Fortymile River assemblage and Lake George assemblage on the south and west sides of Mosquito Flats are interpreted as the same detachment offset by younger high-angle strike slip and dip-slip faults. Similar detachments were documented by Twelker and others (2021) between the YTT Ladue River and Klondike assemblages and the pNA Lake George assemblage. It is unclear if these low-angle detachments are reactivating older thrust faults. Similar low-angle extensional structures have been proposed within the pNA Lake George assemblage elsewhere in eastern Alaska, for example the Salcha River gneiss dome (Pavlis and others, 1993).

High-angle northwest- and northeast-striking faults and lineaments cross cut mid-Cretaceous and earlier low-angle structures throughout the Yukon Tanana Uplands and adjacent parts of Yukon. Northwest-striking structures, such as the Teslin fault, Big Creek fault, and the Coffee Creek fault are more prominent in Yukon. Northeast-striking structures are more common in eastern Alaska, though shorter segments have been mapped in Yukon, such as the Dip Creek fault (Sanchez and others, 2014). The northeast-striking faults generally crosscut the northwest-striking faults in eastern Alaska and are therefore interpreted as

being younger. Many of these high-angles structures bound small basins containing mid-to-Late Cretaceous sediments, Late Cretaceous volcanics, or are intruded by Late Cretaceous to Paleogene intrusions, suggesting the high-angles structures developed in the mid-to-Late Cretaceous. The initial motion on many of these structures may have been dip-slip, resulting in northeast-striking blocks of variable uplift. The Sixtymile Butte area, which preserves mid-Cretaceous volcanic rocks, and the Mount Veta block, with deeply exhumed mid-Cretaceous plutons (Dusel-Bacon and others, 2016), are examples of variably uplifted blocks separated by the Kechumstuk fault (Day and others, 2007, 2014).

The Cenozoic right-lateral Denali and Tintina faults currently bound the northeast and southwest sides of the region. The northeast-striking faults in the Yukon Tanana Upland have been interpreted to link these two major dextral faults with left-lateral oblique motions (Day and others, 2014). It is unclear how much sinistral strike-slip motion is the result of reactivating earlier northeast-striking faults versus development of new structures in the Cenozoic.

DESCRIPTION OF MAP UNITS

SEDIMENTARY ROCKS

CzKs SEDIMENTARY ROCKS, UNDIFFERENTIATED (CENOZOIC TO CRETACEOUS)—A mixed unit of poorly-sorted, volcaniclastic to siliciclastic conglomerate and sandstone, with subordinate amounts of mudstone and siltstone. Both matrix-supported and clast-supported layers were observed. Clasts vary from subangular to rounded. Conglomerate grain size varies between locations, with cobbles commonly up to 20 cm and rare boulders up to 1 m in diameter. Volcanic clasts include andesite, dacite, rhyolite, and felsic tuff. Metamorphic clasts include schist, gneiss, and quartzite. The matrix ranges from poorly sorted brown tuffaceous silt to fine-grained plagioclase- and quartz-rich sand and silt. Sandstones are typically fine- to medium-grained, poorly-sorted, finely-laminated, and poorly to moderately indurated. Sandstones near Cretaceous volcanic or granitic units are commonly dominated by clasts of these lithologies. The unit has low to moderate magnetic susceptibility with a range of 0.02–1.9 x 10^{-3} Système international (SI), with an average of 0.20 x 10^{-3} SI. The unit has variable depositional relationships with mid-Cretaceous, Late Cretaceous, and Paleogene volcanic rocks and therefore must include sediment of variable ages with similar appearance. Significant portions of the sediments appear to lie stratigraphically beneath Late Cretaceous volcanic rocks and are likely correlative with the Indian River Formation in Yukon, which also consists of mixed conglomerates and sandstones that lie stratigraphically below the Late Cretaceous Carmacks volcanic group (Lowey and Hills, 1988; Yukon Geological Survey, 2019). This correlation is supported by a conglomerate exposure in the Mount Fairplay area, which yielded a mid-Cretaceous detrital zircon maximum deposition age (MDA) (19AW206; Twelker and O'Sullivan, 2021) and is overlain by Late Cretaceous volcanic rocks. Other sedimentary exposures include volcanic clasts apparently eroded from the Late Cretaceous volcanic units lKiv, lKav, and lKfv in the map area. Two volcaniclastic samples in the map area yielded Late Cretaceous detrital zircon MDAs of 69 Ma (21RN401) and 70 Ma (21ET094) (Gavel and others, 2023), suggesting deposition after eruption of Late Cretaceous volcanic rocks. Separation of pre-and post-Late Cretaceous sedimentary units was not possible at this map scale with current datasets. This unit also may include deposits as young as Miocene (Foster and Igarashi, 1990).

VOLCANIC ROCKS

Per RHYOLITE (PALEOGENE)—One locality north of the Mosquito Fork bridge with poorly exposed, very fine-grained rhyolitic tuff, likely an airfall deposit, overlying gabbro/diabase of unit Peg, indicating a maximum age of 58 Ma (Werdon and others, 2001). The tuff was described in the field

as extremely friable and powdery. The unit is likely correlative to unit PEr in the Ladue River area near the Alaska-Yukon border (Twelker and others, 2021), though sample 99MBW095B (Szumigala and others, 2002a) from the Taylor Mountain map area contains much higher Sr and Ba than is characteristic of unit PEr in the Ladue River area (Wypych, 2021).

lKav ALKALINE VOLCANIC ROCKS (LATE CRETACEOUS)—Exposures up to 5 sq km ranging from porphyritic trachybasalt to trachyte at several different locations. Based on analyzed samples, the unit is approximately 40 percent trachybasalt and basaltic trachyandesite, 50 percent trachyandesite, and 10 percent trachyte. Based on absence of clasts, all the exposures in the map areas are flows or subvolcanic intrusions, although tuffs and breccias with similar compositions are seen in nearby exposures around Mount Fairplay (Twelker and others, 2021). The rocks are dark colored in shades of gray to brown and weather to light gray or reddish brown and are porphyritic. Trachybasalt contains 3-10 percent olivine (variably altered to serpentine and iddingsite), 3–25 percent augite, 0–3 percent phlogopite, 25–30 percent plagioclase, 2–8 percent alkali feldspar, 2–4 percent opaque minerals, and 30–50 percent glass, variably altered to fine-grained chlorite and calcite. The rocks typically contain 15–30 percent medium-grained phenocrysts (mostly mafic minerals and some plagioclase) in a fine-grained groundmass. Basaltic trachyandesite is similar but contains less augite and appreciable orthopyroxene. Trachyandesite contains 0–5 percent augite, 0–3 percent hornblende, 0–3 percent biotite, 15–40 percent plagioclase, 5–25 percent, 2–3 percent opaque minerals, 0–2 percent quartz, and 20–40 percent fine-grained, intergrown calcite, chlorite, and kaolinite, presumably representing altered glass. These rocks are typically 10–20 percent medium-grained phenocrysts in a fine-grained, feldspathic groundmass. Trachyte is similar but contains more alkali feldspar and less plagioclase. All these rocks are hydrothermally altered, typically with 3–15 percent calcite plus associated phyllosilicates. The magnetic susceptibility of these rocks is variably high, 0.1–19 x 10^{-3} SI (average 6 x 10^{-3} SI). Trachybasalt and basaltic trachyandesite (average 7.5 x 10^{-3} SI) are higher than trachyandesite (average 5.4 x 10^{-3} SI), which is higher than trachyte (average 5 x 10^{-3} SI). The age assignment is based on correlation with Late Cretaceous alkalic volcanic rocks exposed around Mount Fairplay (Twelker and others, 2021). Additionally, a trachyte sample with similar texture and chemistry from unit Kv in the Northeast Tanacross map area yielded a late Cretaceous (67.7 ± 0.9 Ma) U-Pb crystallization age (Todd and others, 2019; Wypych and others, 2021).

lKfv FELSIC VOLCANIC ROCKS (LATE CRETACEOUS)—Predominantly rhyolite-composition extrusive and hypabyssal intrusive rocks with minor dacitic tuff, present in at least seven small (1.6–5.4 sq km) areas to the west and southwest of Mosquito Flats as well as isolated locations south of the Taylor Mountain Batholith. The map unit also includes a more than 70-meter-thick rhyolite tuff in the upper reaches of Gold Creek, which was described as outfall tuff of the Middle Fork Caldera by Bacon and others (2014). The isolated volcanic rocks could represent remnants of an extensive welded tuff. The mapped bodies appear to overlie mid-Cretaceous plutons and older metamorphic rocks. Sample compositions are 10 percent dacite and 90 percent rhyolite. Most of the rocks are pale colored, either white or various shades of pink, gray, brown, orange, or green. Rhyolitic tuff includes crystal tuff and lithic-crystal tuff, which typically contain 10–40 percent crystals, many broken, and 0–25 percent lithic clasts. In most cases they are groundmass-rich, with 70–85 percent microcrystalline groundmass. An uncommon variety contains as little as 35 percent groundmass. Mineralogy includes 5–15 percent quartz, 5–25 percent feldspar, and 4–7 percent biotite (partly to largely replaced by muscovite + chlorite). Dacite tuffs are similar but contain up to 10 percent augite + orthopyroxene (partly replaced by iddingsite) instead of biotite and up to 1.5 percent opaque minerals. Minor rhyolites either have granular to granophyric groundmass, suggestive of a hypabyssal

intrusive origin, or are so strongly altered to kaolinite-quartz-sericite that original textures cannot be deciphered (about one-quarter of the samples). Given their limited occurrence in the unit, they are likely subvolcanic dikes or sills. Strongly altered samples are common and even the least altered samples contain several percent sericite + chlorite + epidote. The unit has much lower magnetic susceptibility than similar felsic tuffs of Sixtymile Butte; measured susceptibility ranging from 0.01–8 x 10^{-3} SI (average 0.5 x 10^{-3} SI). Tuffaceous samples (average 0.8 x 10^{-3} SI) are more magnetic than non-tuffaceous samples (average 0.1 x 10^{-3} SI), probably reflecting the greater degree of hydrothermal alteration experienced by the latter group. The Late Cretaceous age is constrained by zircon U-Pb ages of 68.3 ± 1.4 Ma from a dacite crystal tuff near Kechumstuk Mountain (21DFA047 in Gavel and others, 2023) and 71.1 ± 0.5 Ma from a welded tuff in upper Gold Creek (71AFr965 in Bacon and others, 2014).

lKiv INTERMEDIATE VOLCANIC ROCKS (LATE CRETACEOUS)—Andesite, with lesser basaltic andesite and dacite, mostly as flows or possibly subvolcanic intrusions, with minor andesitic tuffs. These rocks are dark-colored, usually gray, locally purple or red-brown. One large (60 sq km) exposure is present northeast of Mosquito Flats and smaller exposures are mapped along the West Fork of the Dennison Fork River west of the Taylor Highway. These exposures may represent remnants of the same volcanic center or two separate centers. Only one sample (of 23) is volcaniclastic; the others lack clasts and appear to be flows, based on the microcrystalline groundmass. Assuming sub-horizontal layering, this unit is at least 200 meters thick. Andesite is pyroxene-plagioclase phyric (0.5–3 mm) or pyroxene-phyric, with 0.03–0.2 mm plagioclase needles, commonly with sub-parallel orientations, in the groundmass. Typical samples contain 20–35 percent phenocrysts. The groundmass is commonly isotropic or near-isotropic dark colored glass with embedded plagioclase or microcrystalline plagioclase-rich intergrowths. Typical mineral abundances include 5–6 percent augite, 4–8 percent orthopyroxene (partly altered to iddingsite and commonly rimmed by augite), 30–45 percent plagioclase, 30–40 percent glass, 0–10 percent sanidine, and 1–3 percent opaque minerals (with titanomagnetite more abundant than ilmenite). Basaltic andesite lacks sanidine and contains more pyroxene; dacite contains additional quartz and hornblende. Hydrothermal alteration in all samples is weak, generally restricted to dusting of plagioclase by sericite and minor replacement of orthopyroxene by iddingsite. The rocks are moderately magnetic, with magnetic susceptibility of 4–22 x 10^{-3} SI (average of 12 x 10^{-3} SI). The values vary with rock type with average values of 13.2, 12.3, and 10.4 x 10^{-3} SI for basaltic andesite, andesite, and dacite, respectively. The absence of values less than 4 x 10^{-3} SI is likely due to limited hydrothermal alteration. The basis for the Late Cretaceous age is the correlation with intermediate composition, sub-alkalic rocks of the Northeast Tanacross map area (approximately 30 km to the east), where a dacite yielded a whole-rock $^{40}Ar/^{39}Ar$ plateau age of 65.5 ± 0.4 Ma (Naibert and others, 2018) and an andesite yielded a U-Pb zircon crystallization age of 71.5 ± 3.0 Ma (Todd and others, 2019; Wypych and others, 2021). This unit overlies or is in fault contact with metamorphic rocks of the Chicken assemblage, the Fortymile River assemblage, and plutonic rocks of the Taylor Mountain batholith. The unit is distinguished from similar age volcanic rocks of unit lKav, which have more alkaline compositions, have experienced a greater degree of hydrothermal alteration, and consequently have variable magnetic susceptibility.

Kimv INTERMEDIATE TO MAFIC VOLCANIC ROCKS (MID-CRETACEOUS)—This unit includes aphanitic to porphyritic andesite, trachyte, trachyandesite, and trachybasalt. The unit lies above, is interlayered with, or has ambiguous contact relationships with the mid-Cretaceous West Fork tuff (Kwff). A phlogopite sample from trachybasalt station 21RN530 yielded a $^{40}Ar/^{39}Ar$ age of 100.8 ± 0.3 Ma (Naibert and others, 2023). Trachybasalt and trachyandesite samples have intense

calcite-chlorite alteration and include 3–40 percent phenocrysts of phlogopite or biotite, which are partially or largely altered to chlorite and muscovite, and lesser phenocrysts of plagioclase, alkali feldspar, quartz, and opaques. Very fine groundmass includes plagioclase needles, partially altered to sericite, and lesser glass. This unit has a moderate to high magnetic susceptibility, 0.45–19.1 x 10^{-3} SI and averaging 8.2 x 10^{-3} SI. The volcanic rocks within this unit are very similar to Late Cretaceous intermediate volcanics and alkaline volcanics described above and are differentiated by their contact relationships with and proximity to Kwff and the 100.8 Ma $^{40}Ar/^{39}Ar$ age, though unit assignment remains questionable for undated stations.

Kwff WEST FORK FELSIC TUFF (MID-CRETACEOUS)—Rhyolitic to dacitic tuff and subordinate rhyolite to dacite flows south of the West Fork Dennison Fork River and surrounding the Mount Fairplay area. The unit is predominantly light tan, with lesser gray, pale green, pale yellow, or maroon colors. Tuff weathers brown, orange, or greenish maroon. The tuffaceous lithologies are matrix-supported, moderately sorted, crystal-rich, and contain up to 10 percent lithic fragments up to 50 mm in diameter. The crystal fraction is euhedral, often fragmented, and commonly includes around 3 percent quartz, locally up to 25 percent; around 6 percent feldspar, locally up to 15 percent; up to 2 percent biotite is present in some samples, and hornblende occurs rarely. Other minerals include disseminated pyrite and hematite. Lithic fragments consist of very fine-grained, subangular volcanic rocks, flattened pumice fragments, and lapilli. Rarely observed alterations include sericite, clay, or propylitic alteration and potassium (K) enrichment. Volcanic flows are locally laminated and are typically porphyritic, having around 3 percent (locally up to 30 percent) alkali feldspar phenocrysts, 1 to 2 percent quartz phenocrysts, and 1 to 3 percent disseminated, oxidized pyrite, 1 percent hematite, and up to 90 percent aphanitic groundmass. Secondary pyrite mineralization and argillic or sericitic alteration were observed locally. This unit has a low to moderate magnetic susceptibility, ranging from 0.02–8.96 x 10^{-3} SI and averaging 1.51 x 10^{-3} SI. Two samples yield U-Pb zircon crystallization ages of 107.6 ± 2.1 and 108.7 ± 2.2 Ma (21TJN180 and 21MLB006; Gavel and others, 2023), and a tuff from the Eastern Tanacross map area yielded a 107.9 ± 0.3 Ma zircon crystallization age (19TJN299; Wildland and others, 2021). Bacon and others (1990) interpreted this unit as one of several remnant volcanic calderas in the region, though an alternative interpretation is that the West Fork tuff is an outfall tuff from the Sixtymile Butte caldera to the southwest, due to their similar ages and compositions.

Ksfv SIXTYMILE BUTTE FELSIC VOLCANIC ROCKS (MID-CRETACEOUS)—Mostly rhyolite tuff with lesser dacite tuff and hypabyssal felsic intrusions, which occur over a 215-sq-km area in the south-central part of the Western Tanacross map. Bacon and others (1990) considered this near-circular volcanic field to represent intracaldera volcanics plus local outflow ignimbrites. Assuming sub-horizontal bedding, this unit is at least 550 m thick. It apparently overlies metamorphic rocks of the Lake George assemblage. Rocks of this unit are generally pale gray, pinkish-gray, or greenish-gray and commonly weather brown, purple, or orange. Based on 120 collected samples, approximately 15 percent of the unit is felsic hypabyssal (sub-volcanic) and 85 percent is extrusive. Based on the presence of lithic clasts and variably broken crystals, the extrusive rocks are entirely lithic-crystal and crystal-lithic welded tuffs. Approximately 10 percent of the tuffs have dacitic compositions, 80 percent rhyolitic, and 10 percent lack compositional data. The tuffaceous rocks contain 10–45 percent crystals, many broken, usually with more feldspar than quartz. They also contain 5–50 percent lithic (usually rhyolitic) clasts and locally fiamme. Crystal contents include 5–20 percent feldspar, 5–25 percent quartz, 0–5 percent biotite (partly to largely replaced by chlorite), trace hornblende, and 0.5–3 percent opaques. Dacite tuffs are similar but contain less quartz and up to 8 percent augite.

Groundmass is microcrystalline quartz-feldspar-muscovite intergrowths and locally have spherulitic textures. Hydrothermal alteration is ubiquitous, as sericite-calcite-chlorite partial replacement of plagioclase phenocrysts, mafic minerals, and groundmass. Hypabyssal intrusions are usually biotite granite porphyry, rarely hornblende granodiorite porphyry. These rocks occur sporadically near the margins of the inferred caldera, as noted by Bacon and others (1990). They comprise 5–20 percent phenocrysts (typically 0.5–2 mm) in a microcrystalline (typically granular to granophyric, locally graphic) groundmass. Quartz is commonly skeletal or embayed and locally in glomerocrystic clusters. Hydrothermal alteration is variably intense; in some rocks the groundmass is almost entirely altered to kaolinite, but usually the plagioclase, mafic minerals, and groundmass are at least partly altered to calcite-chlorite-sericite. The magnetic susceptibility of this unit is variable, 0.03–21 x 10^{-3} SI, averaging 3 x 10^{-3} SI. Average values for intrusive (3.3 x 10^{-3} SI) and extrusive (2.8 x 10^{-3} SI) samples are practically identical, however dacite tuff (10.5 x 10^{-3} SI) is significantly higher than rhyolite tuff (2 x 10^{-3} SI). Zircon from two samples (20ADW001 and 21SPR026) of rhyolite tuff from this unit yielded identical U-Pb ages of 108.4 ± 2.2 Ma (Gavel and others, 2023). This is within error of the 107.9 ± 0.3 Ma age reported for the West Fork felsic tuff (Wildland and others, 2021).

INTRUSIVE ROCKS

PEfp FELSIC HYPABYSSAL INTRUSIONS (PALEOGENE)—Dikes and small intrusions of felsic porphyry and lesser granite, with phenocrysts up to 30 mm in an aphanitic matrix. The phenocrysts include up to 40 percent quartz, up to 40 percent alkali feldspar, up to 20 percent plagioclase, 3 percent magnetite, 2 percent other opaque minerals, 1 percent biotite, and minor muscovite. Matrix is glassy (50 to 100 percent devitrified), and in some cases recrystallized. Phenocrysts are euhedral to subhedral. Some samples have sparse, disseminated or veinlet-hosted pyrite, and vuggy quartz veins with disseminated pyrite weathering to iron oxides. Magnetic susceptibility of this unit varies between 0.01 and 0.54, with an average of 0.22 x 10^{-3} SI. Zircon from dikes north of Gold Creek within the Taylor Mountain map area yielded U-Pb ages of 56.9 ± 1.1 and 56.2 ± 1.1 Ma (Gavel and others, 2023). Zircon from two samples of this unit in the nearby Ladue River area yielded ages of 57.1 ± 1.2 and 58.6 ± 1.4 Ma (samples 19KS100 and 19ET277; Wildland and others, 2021). The equivalent unit in Yukon, the North Ladue River porphyry, yielded a U-Pb zircon age of 58.3 ± 0.5 Ma (Yukon Geological Survey, 2020). This unit is of similar age and composition to Paleogene rhyolite in eastern Alaska and similar age to the Rhyolite Creek volcanic rocks in Yukon (Yukon Geological Survey, 2019).

PEg GABBRO/DIABASE (PALEOGENE)—Description from Werdon and others (2001). Fine- to medium-grained (1–5 mm) tholeiitic microgabbro or diabase. Typical mineralogy is 50–70 percent felted plagioclase laths, 30–50 percent altered clinopyroxene + olivine, 3–5 percent magnetite + ilmenite, and 0–3 percent biotite. Although previously mapped as fine- to coarse-grained basalt (Foster, 1976), the absence of columnar jointing, layering, vesicles, volcanic breccias, or other evidence of extrusive character suggests that this unit is predominantly of shallow (?) intrusive origin or the interior portion of a thick flow. Contacts with adjacent units, where exposed, are high-angle and sheared, suggesting faulted intrusive contacts. $^{40}Ar/^{39}Ar$ biotite plateau age of 57.5 Ma (Werdon and others, 2001). Probably correlates with Paleogene basalts of similar major- and trace-element compositions (within-plate) throughout Interior Alaska. Relatively unaltered mafic dikes (too small to be shown at map scale) are sporadically present elsewhere in the map area and probably represent the same Paleogene magmatism. Magnetic susceptibility of the unit is moderate to high, usually 1–11 x 10^{-3} SI. Large bodies spatially correspond to aeromagnetic lows, indicating they are reversely magnetized, similar to Paleogene basalt in the Fairbanks area (Roe and Stone, 1993).

lKm MONZONITE (LATE CRETACEOUS)—Several small (1.6–4 sq km), irregular bodies of principally monzonite (with minor monzodiorite and quartz syenite) occur just south of the Sixtymile Butte volcanic field (Ksfv). They are in high-angle fault contact with Ksfv, appear to intrude late Cretaceous alkalic volcanic rocks (lKav) and have unclear contact relationships with Lake George assemblage metasedimentary rocks and unmetamorphosed sedimentary rocks. These are dark-colored rocks most recognizable by their distinctive alkalic chemical compositions, with 50–54 percent SiO_2, 6–9 percent $Na_2O + K_2O$, and higher proportion of K_2O than Na_2O (Wypych and others 2022a). Monzonite is typically porphyritic, with coarse augite, olivine, and orthoclase phenocrysts in a fine-grained biotite-plagioclase matrix or coarse augite and olivine in a fine-grained alkali feldspar-plagioclase matrix. Typical mineralogy includes 15–25 percent olivine (partly altered to serpentine and iddingsite), 10–15 percent augite, 0–3 percent biotite, 30 percent alkali feldspar, 25–30 percent plagioclase, 1 percent apatite, and 2–3 percent magnetite + ilmenite. The assigned late Cretaceous age is based on regional correlation and intrusive relations with Late Cretaceous volcanics (lKav). The monzonite strongly resembles—in mineralogy and composition—Late Cretaceous augite-olivine monzonite of the Mount Fairplay complex (Newberry, 2020), 25 kilometers to the east and thus we assign this unit to the Mount Fairplay plutonic suite. The unit has low to moderate magnetic susceptibility, with a range of 0.08 to 7.0 x 10^{-3} SI (average 3.8 x 10^{-3} SI).

lKgd GRANODIORITE TO QUARTZ DIORITE (LATE CRETACEOUS)—Several small (0.9–8 sq km) bodies of moderately magnetic quartz diorite to granodiorite. These bodies appear to intrude mid-Cretaceous granite and metamorphic rocks of the Lake George assemblage. Based on collected samples, more than half of the rocks are quartz diorite, quartz monzodiorite, or tonalite; the remainder are granodiorite. Both types contain little hornblende or titanite. Fine-grained, seriate to sub-equigranular pyroxene-biotite quartz diorite is the most common rock type of the unit. It contains 55–65 percent plagioclase, 7–10 percent quartz, 1–4 percent alkali feldspar, 5–7 percent augite, 2–3 percent enstatite, 13–15 percent biotite, 3–6 percent opaque minerals (about twice as much magnetite as ilmenite), and 0.5–1 percent apatite. Quartz monzodiorite is similar but contains more quartz (10–15 percent) and alkali feldspar (10–15 percent) with less plagioclase (40–45 percent). Tonalite contains more than 20 percent quartz, little alkali feldspar, and less pyroxene. Hornblende-biotite granodiorite is commonly fine- to medium-grained seriate, but is also fine- to coarse-grained porphyritic, with coarse quartz and plagioclase in a fine-grained groundmass. Typical mineralogy includes 40–50 percent plagioclase, 20–30 percent quartz, 15–20 percent alkali feldspar, 10–12 percent biotite, 2–6 percent hornblende, 0.3–1 percent opaques (principally magnetite), 0.3–0.5 percent apatite, and trace titanite. The rocks of this unit characteristically display little hydrothermal alteration: slight replacement of pyroxene by actinolite, biotite by chlorite, and plagioclase by sericite. The unit has moderately high magnetic susceptibility between 6.5 to 29.9 x 10^{-3} SI (average 19 x 10^{-3} SI). Despite similarities in magnetic susceptibility and composition, rocks of this unit are distinguished from rocks of the Taylor Mountain batholith based on the near-absence of titanite and only minor hydrothermal alteration; epidote is conspicuously absent. The age assignment is based on zircon from quartz monzodiorite (21WCW008) with a U-Pb age of 71.1 ± 1.4 Ma (Gavel and others, 2023). This unit is correlated with the Late Cretaceous Pika diorite of Wypych and others (2021), located about 30 km to the east and we assign it to the Taurus plutonic suite. It has a similar range of compositions (mostly quartz diorite to granodiorite), pyroxene-biotite + hornblende mineralogy, magnetic susceptibility (average 20 x 10^{-3} SI), and age (zircon U-Pb of 70.3 ± 0.5 Ma; Todd and others, 2019).

Kpg PORPHYRYTIC GRANODIORITE DIKES (CRETACEOUS?)—Biotite- and hornblende-bearing porphyritic dikes with granodioritic composition, 2–15 mm phenocryst grain size, 15 percent feldspar phenocrysts, 30 percent quartz phenocrysts, 5 percent biotite, 5 percent amphibole, and 45 percent fine-grained groundmass. The dikes intrude the Chicken assemblage north of the mouth of Gold Creek. These dikes are less silicic overall, include hornblende, and contain fewer quartz phenocrysts than the nearby dated Paleogene felsic intrusions (Pfp). It is likely that these dikes are related to a nearby mid-Cretaceous Granodiorite body (Kgd).

Kgd GRANODIORITE (MID-CRETACEOUS)—Biotite-bearing granodiorite and lesser quartz monzodiorite and quartz monzonite, which outcrops in small plutons and wide-spread dikes mainly in the southern part of the Western Tanacross project. The unit is typically equigranular to seriate, hypidiomorphic, and less commonly porphyritic. Grain size typically varies from 0.1 to 15 mm, with rare megacrysts up to 60 mm. Mineralogy consists of 25–50 percent plagioclase, 10–45 percent quartz, 10–45 percent alkali feldspar, 5–15 percent biotite, 0–20 percent hornblende, 1–2 percent magnetite, and trace titanite. Both biotite and hornblende are locally chloritized. Hornblende surrounds rare augite crystals in thin section. Magnetic susceptibility of this unit is relatively high, varying between 2.0 and 42.8 x 10^{-3} SI and averages 19.4 x 10^{-3} SI. Zircon from similar granodiorite in the Ladue River area yielded U-Pb ages of 104.2 ± 2.3 and 107.7 ± 2.3 Ma (Wildland and others, 2021). This unit is assigned to the Gardiner Creek plutonic suite.

Kgp GRANITE PORPHYRY (MID-CRETACEOUS)—Granite porphyry with lesser porphyritic granite and granodiorite porphyry, present as both dikes (approximately 60 percent of occurrences) and large hypabyssal intrusions (approximately 40 percent of occurrences). We assign this unit to the Mount Harper plutonic suite. At least 10 hypabyssal bodies are present, each 1–45 sq km in area, with a total of about 150 sq km around Mosquito Flats. Based on 251 samples, 78 percent of the rocks are granite, 10 percent are granodiorite, and 2 percent are trondhjemite (10 percent of samples lack compositional data). Samples from dikes mostly resemble those from larger intrusions, though dike samples display a wider range of phenocryst abundances (5–65 percent) than do pluton samples (mostly 15–25 percent phenocrysts). Dike samples commonly display less intense hydrothermal alteration with 3–8 percent sericite + chlorite + epidote + calcite versus 5–12 percent sericite + chlorite + calcite in pluton samples. Groundmass in pluton samples tends to be coarser (0.05–0.1 mm) and more micrographic; groundmass in dikes is finer-grained (0.02–0.07 mm) and granular-granophyric-spherulitic. The mineralogy of both is similar, with 10–35 percent plagioclase (partly to strongly altered), 10–45 percent alkali feldspar, 15–35 percent quartz, 5–10 percent biotite (mildly to strongly replaced by chlorite + muscovite), 0–1 percent hornblende (variably altered to epidote-chlorite), and 0.5–1 percent opaque minerals (variably replaced by hematite-limonite). Quartz variably displays resorption textures; the other phenocryst minerals are subhedral. Granodiorite porphyry is similar but contains less alkali feldspar (5–20 percent) and more hornblende (5–10 percent, variably altered). Samples with trondhjemite (Na-rich) compositions probably represent relatively rare sodic alteration, as these invariably also contain a significant secondary assemblage of chlorite-sericite-epidote-calcite. All samples examined display at least minor hydrothermal alteration (sericitic and/or propylitic); many are intensely altered. Magnetic susceptibility is variable but mostly low (0.01–31.6 x 10^{-3} SI; average 1.0 x 10^{-3} SI), with variation largely related to degree of hydrothermal alteration. Average values for dikes (2 x 10^{-3} SI) are higher than those for intrusions (1 x 10^{-3} SI), probably related to more intense alteration in intrusive samples. Finally, granodiorite porphyry has higher values (average 5.5 x 10^{-3} SI) than do granite (0.8 x 10^{-3} SI) or trondhjemite (0.6 x 10^{-3} SI).

The Cretaceous age is indicated by zircon U-Pb ages in the map area from both granite porphyry and granodiorite porphyry dikes (21ET119, 110.8 ± 2.2 Ma; 21RN094, 109.8 ± 2.2 Ma; 21RN282, 107.2 ± 2.2 Ma)(Gavel and others, 2023). Dikes intrude unit Kg and metamorphic rocks of the Lake George assemblage. Larger plutons display ambiguous relations with Kg, intrude Lake George assemblage rocks, and are in fault contact with Fortymile River assemblage metamorphic rocks. Overlap in U-Pb zircon ages from the West Fork rhyolite tuff and Sixtymile Butte felsic volcanic units (Kwff and Ksfv) suggests that this unit is contemporaneous with felsic volcanism.

Kgb GABBRO (MID-CRETACEOUS)—One small intrusion within the Chicken assemblage to the east of Diamond Mountain. The unit includes pyroxene gabbro and orbicular clinopyroxene cumulate with mid-Cretaceous zircons (Todd, personal communication, 2022). No similar rocks were observed elsewhere in the map area.

Kg GRANITE (MID-CRETACEOUS)—Tan, white, or light gray to pale pink, seriate to equigranular biotite-bearing granite with minor amounts of granodiorite. We assign this unit to the Mount Harper plutonic suite. Typically the granite has grain size of 0.1 to 10 mm, 10 to 35 percent alkali feldspar, 15–55 percent plagioclase, 25–40 percent quartz, 0–20 percent biotite, 0–2 percent titanite, and locally up to 3 percent white mica, 2 percent epidote, and 1 percent garnet. Biotite is slightly to moderately chloritized, especially near pluton contacts. Plagioclase is often partially altered to sericite. The unit is generally fresh to partially weathered. Pegmatite dikes of similar composition occur throughout the map area, with up to 50 mm long euhedral alkali feldspar crystals in a matrix of 10 mm quartz and plagioclase, and up to 10 percent muscovite. Aplite dikes are light gray and equigranular, with grain sizes of 0.5–2 mm. Magnetic susceptibility is variable, 0.02–50.2 x 10^{-3} SI and averaging 3.24 x 10^{-3} SI. The variation is not systematically related to equigranular, seriate, or pegmatitic texture. A zircon U-Pb age from sample 21ET193 is 110.0 ± 2.2 Ma (Gavel and others, 2023). Zircon U-Pb ages from granite in the neighboring Northeast Tanacross and Ladue River–Mount Fairplay map areas range are ca. 106.7–114.1 Ma (Wypych and others, 2020; Wildland and others, 2021). On the eastern edge of the Tanacross D-1 Quadrangle, the granite extends into Yukon, Canada, where it is mapped as the ca. 110–109 Ma Crag Mountain pluton; part of the Whitehorse Plutonic suite (Yukon Geological Survey, 2019).

Jg NAPOLEON CREEK PLUTONIC SUITE UNDIVIDED (JURASSIC)—Undivided unit consisting of multiple Early Jurassic intrusions, including a composite 100-sq-km-diameter pluton north of Mosquito Flats, a smaller body directly south of that main body, and multiple plutons in the southern Eagle Quadrangle near Chicken, Alaska. These Early Jurassic plutons correlate with plutons to the northeast in the Chicken area (Werdon and others, 2001) and with plutons to the northwest that have U-Pb zircon ages of 181–191 Ma (Day and others, 2014). The plutons include a variety of igneous rock types and we herein refer to all Early Jurassic intrusions in the map area as the Napoleon Creek Plutonic suite, after the Napoleon Creek pluton described by Werdon and others (2001) in the Eagle A-2 Quadrangle. The majority of the plutons are characterized by alkalic geochemical compositions, ranging from syenite and quartz syenite to quartz monzodiorite, and approximately a quarter of the rocks have granodiorite to granite compositions. Unlike farther east (Eagle A-2; Werdon and others, 2001) and north (Eagle A-4 and A-5; Day and others, 2014) where separate quartz-rich and quartz-poor bodies occur, the two types are often intermixed in the Western Tanacross and Taylor Mountain map areas. Rocks of this unit appear to intrude the older Taylor Mountain suite and metamorphic rocks of the Chicken and Fortymile River assemblages. Quartz-poor members of this unit include (biotite)-augite-hornblende syenite, (biotite)-hornblende quartz syenite, biotite-hornblende quartz monzonite, and

biotite-hornblende quartz monzodiorite, of which the former is most abundant. These rocks invariably possess porphyritic textures, with alkali feldspar megacrysts in a medium- to coarse-grained hornblende-rich groundmass and usually display minor to moderate propylitic alteration. Shear or foliation textures are present in 10–20 percent of the rocks. Typical mineral abundances are 0–5 percent biotite, 0–5 percent augite, 7–40 percent hornblende, 2–15 percent quartz, 20–55 percent alkali feldspar, and 12–55 percent plagioclase. Trace minerals include 0.5–1 percent opaque minerals, 0.5–1 percent apatite and invariably 1–2 percent titanite. Quartz-rich plutonic rocks include biotite-hornblende granodiorite, hornblende-biotite granite, biotite granite, and biotite granite aplite. These rocks are typically fine- to medium-grained, but medium- to coarse-grained types are also present. Quartz content ranges from 20–40 percent and other minerals vary with rock type. Granodiorite invariably contains both hornblende and biotite. The rocks display major to minor amounts of propylitic alteration. Magnetic susceptibility is usually moderate: 0.05–10 x 10^{-3} SI (average 4.5 x 10^{-3} SI) for quartz-rich rocks and slightly higher, 0.3–40 x 10^{-3} SI (average 7.7 x 10^{-3} SI) for quartz-poor rocks. U-Pb crystallization ages in the map area (Gavel and others, 2023) include 185.4 ± 3.7 Ma (granodiorite, 21AW136), 184.8 ± 3.7 Ma (granite, 21ET227), 183.8 ± 3.7 Ma (quartz syenite, 21MLB187), 191.1 ± 3.8 Ma (syenite, 21AW180), and 191.3 ± 0.4 Ma (granite near Mount Warbelow; Dusel-Bacon and others, 2009) indicating near-simultaneous intrusion of the quartz-rich and quartz-poor intrusions.

Taylor Mountain Plutonic Suite

The Taylor Mountain Batholith is a large (780 sq km) composite batholith of Late Triassic age with several smaller related bodies to the west at Diamond Mountain and near Kechumstuk Mountain. The batholith is associated with a significant magnetic anomaly on airborne geophysical surveys (Emond and others, 2015; Burns and others, 2015). The magnetic anomaly extends under the Mosquito Flats, which we interpret to be buried Taylor Mountain suite intrusions. The plutons include gabbro (primarily on the west, north-central, and southeast margins of Taylor Mountain), diorite, quartz diorite, tonalite, granodiorite, granite, and trondhjemite. Based on 249 collected samples, the Taylor Mountain Batholith is approximately 10 percent gabbro, 15 percent diorite and quartz diorite, 15 percent tonalite, 15 percent granodiorite, 10 percent granite and quartz monzonite, 15 percent trondhjemite, and 20 percent with no chemical analyses. Less-altered felsic and intermediate composition rocks of the plutonic suite always contain the assemblage magnetite + titanite, suggesting a relatively high magmatic oxidation state. Epidote is ubiquitous, some of which is texturally primary, suggesting a moderate depth of emplacement between 10–18 km depth (0.3–0.5 GPa; Schmidt and Thompson, 1996). The Taylor Mountain suite in eastern Alaska is the westernmost exposure of a belt of late Triassic magmatic rocks, which stretch into western Yukon and continue in the Stikine Terrane in British Columbia. The plutonic suite appears to intrude rocks of the Chicken assemblage. The Taylor Mountain Batholith also appears to intrude the Fortymile River assemblage along the southern margin of the batholith. The plutonic suite is intruded by younger Jurassic plutonic rocks.

Ŧtg TAYLOR MOUNTAIN GRANITE (TRIASSIC)—One small mappable area near the south summit of Taylor Mountain containing granite to quartz monzonite. Samples are white and pink to gray, seriate to equigranular, with grain sizes from 0.5–15 mm. Mineralogy includes up to 40 percent plagioclase, up to 45 percent alkali feldspar, up to 25 percent quartz, up to 8 percent biotite, and up to 15 percent hornblende, with up to 1 percent magnetite, titanite, and epidote. The largest phenocrysts are commonly alkali feldspar crystals up to 15 mm, plagioclase and hornblende up to 7 mm, and scattered biotite flakes up to 2 mm. Quartz is often interstitial. Mafic minerals are partially chloritized. Titanite is euhedral and up to 1.5 mm. Clinopyroxene is rarely observed in thin section

as cores of hornblende grains. The granite phase of the Taylor Mountain Batholith has been dated at 214.6 ± 1.8 Ma (Todd and others, 2023). Sharp contacts were not observed with surrounding trondhjemite and granodiorite-tonalite phases, suggesting the phases are gradational. Magnetic susceptibility is moderate to high from 6.3 to 26.5 x 10^{-3} SI and averaging 13.0 x 10^{-3} SI.

Ŧtgd TAYLOR MOUNTAIN GRANODIORITE TO TONALITE (TRIASSIC)—Plutonic rocks dominated by granodiorite and tonalite but also including subordinate compositions ranging from diorite to granite. All compositions contain significant titanite (commonly visible in hand sample) and are slightly to strongly altered to chlorite-epidote-sericite + calcite. Granodiorite and tonalite are always hornblende-bearing and commonly biotite-bearing, weakly to strongly altered, locally foliated, and possess seriate to porphyritic textures. Fine-grained samples are dark to light greenish gray and medium- to coarse-grained samples are greenish black and white. Hornblende is usually more abundant than biotite. Weakly- to moderately-altered granodiorite typically contains 40–50 plagioclase (variably altered), 20–25 percent quartz, 10–15 percent alkali feldspar, 7–15 percent hornblende, 3–8 percent biotite (variably chloritized), 0.5–2 percent titanite (mostly primary based on texture), 0.5–1.5 percent opaques (mostly magnetite), 0.5 percent apatite, 0.1–2 percent chlorite, 0.5–3 percent epidote (some of which appears texturally primary), trace calcite and trace allanite. More strongly altered samples contain up to 20 percent chlorite, 7 percent epidote, and 6 percent calcite, and the primary mafic minerals are often completely replaced. Minor quartz monzodiorite, associated with granodiorite, is similar but contains about 15 percent quartz and up to 1 percent augite. Tonalite contains 3–5 percent alkali feldspar and typically 15–18 percent partly altered mafic minerals. Minor granite contains less plagioclase (typically 30 percent), more alkali feldspar (25–35 percent), and commonly more biotite than hornblende. U-Pb zircon ages from within the Taylor Mountain Batholith range from 213.2 to 204.4 Ma (Jones and O'Sullivan, 2020; Gavel and others, 2023; Todd and others, 2023). U-Pb zircon ages from the Kechumstuk Mountain pluton are ca. 215 Ma (Dusel-Bacon and others, 2009; Dusel-Bacon and others, 2015; Todd and others, 2023) and from the Diamond Mountain pluton range from 208.5 to 201.0 Ma (Dusel-Bacon and others, 2009; Gavel and others, 2023; Todd and others, 2023). Due to the 15 million year span of ages, this unit either represents prolonged magmatism or multiple discrete pulses of magmatism with similar compositions. Internal boundaries within the unit were not identified due to the scale of mapping and limited intact exposures. Magnetic susceptibility varies considerably, 0.1–34.5 x 10^{-3} SI, with a moderately high average of 9.1 x 10^{-3} SI. Rocks of this unit are distinguished from similar-appearing Cretaceous plutonic rocks by higher magnetic susceptibility and presence of significant titanite. Within the map area, this unit intrudes rocks of the Chicken assemblage and Fortymile River assemblage and is overlain by Cretaceous-Tertiary sedimentary rocks.

Ŧtgb TAYLOR MOUNTAIN GABBRO, DIORITE, AND QUARTZ DIORITE (TRIASSIC)—Variably metamorphosed, mostly gabbro and gabbroic greenstone, quartz diorite, and some diorite, with minor olivine clinopyroxenite and hornblendite. Gabbro, gabbroic greenstone, and diorite are all dark colored, fine- to medium-grained rocks. Gabbroic greenstone is fine- to medium-grained and possesses randomly oriented grains partly to completely replaced by greenschist facies minerals. Typical mineralogy in examined thin sections includes 20–40 percent hornblende (partly to completely replaced by actinolite + chlorite), 50–60 percent former plagioclase grains (based on texture) completely replaced by fine-grained clinozoisite + muscovite + albite + calcite, 1 percent secondary titanite, and 3–4 percent opaque minerals (partly replaced by titanite). Gabbro is fine- to medium-grained with mafic minerals that vary from augite-dominated to hornblende-dominated and includes sub-equal amounts of the two. Typical mineralogy includes 55–65 percent plagioclase

(slightly to moderately replaced by clinozoisite), 0–35 percent augite (slightly to mostly replaced by hornblende), 0–30 percent hornblende (trace to slightly replaced by epidote + chlorite), 3–5 percent opaque minerals (ilmenite + magnetite + pyrrhotite), and 0–2 percent secondary titanite. The most augite-rich gabbro also contains 10 percent olivine, partly replaced by talc. Olivine clinopyroxenite is a fine-grained rock with 70 percent diopside, 20 percent olivine (partly altered to serpentine), 7 percent plagioclase, and 3 percent opaques. It is unclear how this rock relates to the surrounding gabbro. Hornblendite was observed on the northern boundary of the Taylor Mountain Batholith. The hornblendite is composed of up to 70 percent hornblende crystals up to several centimeters long, 10 percent plagioclase, and up to 30 percent augite in the cores of hornblende crystals and as finer-grained euhedral crystals with plagioclase. Minor chlorite, epidote, and calcite replace hornblende and plagioclase. Both brecciated and fluid mixing contacts were observed between hornblendite and surrounding diorite to quartz diorite, suggesting that the hornblendite crystallized early, possibly as a cumulate along the northern margin the magma chamber and was repeatedly injected by dioritic magma.

Intermediate composition rocks are mostly fine- to medium-grained, seriate biotite-hornblende quartz diorite with lesser quartz monzodiorite and minor diorite and monzodiorite. These rocks are commonly dark colored, but can also be various shades of gray. Quartz diorite typically contains 50–60 percent plagioclase (variably altered to sericite-epidote), 7–10 percent quartz (typically interstitial and nearly invisible in hand sample), 3–5 percent alkali feldspar (also interstitial), 8–20 percent hornblende (usually little-altered), 1–10 percent biotite (slightly to strongly chloritized), 0.5–2 percent titanite (subhedral to euhedral primary texture), 0.5–2 percent opaques (predominantly magnetite), 0.5–1 percent apatite, 0.5–3 percent chlorite, 1–10 percent epidote (some of which appears texturally primary), trace to 2 percent sericite, and trace to 1 percent (secondary) calcite. Quartz monzodiorite that occurs with quartz diorite contains up to 10 percent alkali feldspar, never more than 10 percent quartz, and can contain up to 2 percent augite. Monzodiorite and diorite are similar but contain up to 12 percent pyroxene (both augite and enstatite), and no more than 3 percent quartz. Contact relationships with more felsic phases are poorly exposed but are likely gradational. Mappable areas of this unit generally occur near the margins of the Taylor Mountain Batholith and in the southern portion of the Kechumstuk Mountain pluton. This unit is variably magnetic, with magnetic susceptibility of 0.1–120 x 10^{-3} SI and averaging 17 x 10^{-3} SI.

Zircon from a sample of gabbroic greenstone (21ADW146) yielded a U-Pb age of 215.6 ± 4.4 Ma (Gavel and others, 2023), consistent with other late Triassic ages determined for the Taylor Mountain batholith (Werdon and others, 2001; Dusel-Bacon and others, 2009). Two other samples, gabbro at 21AW152 and quartz diorite at 21ADW136, yielded zircon U-Pb ages of 201.0 ± 4.0 Ma and 202.2 ± 4.1 Ma, respectively (Gavel and others, 2023). These samples are from the southern margin of the Taylor Mountain Batholith and foliation was observed in both samples.

TAYLOR MOUNTAIN TRONDHJEMITE (TRIASSIC)—Variably altered biotite-hornblende and hornblende-biotite trondhjemite, recognized from chemical analyses using the criteria (e.g., felsic, high Na_2O, low K_2O, moderate CaO) of Barker (1979). These are leucocratic rocks consisting primarily of fine- to medium-grained oligoclase and quartz with minor alkali feldspar, mafics, and magnetite. Typical mineralogy includes 55–60 percent plagioclase (oligoclase, based on microprobe analyses), 20–30 percent quartz, 3–5 percent alkali feldspar, 2–8 percent biotite (variably replaced

by chlorite), 2–8 percent hornblende (usually little altered), 0.5–1 percent titanite (subhedral to euhedral, likely magmatic), 0.5–2 percent magnetite, 0.5–2 percent epidote (some of which is subhedral to euhedral and probably late magmatic), and 0.2–0.5 percent apatite. Additional secondary minerals include 0.5–10 percent chlorite, trace sericite, up to 2.5 percent calcite, and up to 2 percent actinolite. Biotite always displays at least minor alteration to chlorite and plagioclase to sericite + calcite + epidote. Hornblende can be completely unaltered or slightly altered to actinolite + chlorite + epidote. Compositions of hornblende from a least-altered trondhjemite yielded a pressure of 0.36–0.9 GPa, using the Al-in-hornblende geobarometer of Schmidt (1992), consistent with the presence of texturally primary epidote.

Magnetic susceptibility of trondhjemite is moderately high, ranging from 2.7–26.9 x 10^{-3} SI and averaging 10.9 x 10^{-3} SI. More strongly altered rocks yield lower values. Mafic minerals in trondhjemite samples are generally less altered, or at least not more altered, than other parts of the batholith. The trondhjemite composition is therefore interpreted to be primary and not a result of sodic alteration. The age of the unit is based on zircon from a trondhjemite sample in the eastern part of the map area, which yielded a U-Pb age of 211.3 ± 4.2 Ma (21TJN161 in Gavel and others, 2023). The majority of trondhjemite samples were collected from the central part of the Taylor Mountain Batholith. Combined with the ca. 211 Ma age, this spatial pattern implies the unit was a relatively early phase of the batholith. The contact relationships between trondhjemite and other units of the Taylor Mountain Batholith are not well exposed. Multiple trondhjemite dikes interpreted to be part of this unit were observed intruding metamorphic rocks of the Fortymile River assemblage.

Other Intrusive Rocks

Pg MOUNT WARBELOW GRANITE (PERMIAN)—Creamy white to pinkish gray seriate hornblende-biotite granite, weathering gray to orangish brown. The unit consists of 15–40 percent alkali feldspar, 15–35 percent plagioclase feldspar, 15–35 percent quartz, up to 10 percent biotite, up to 4 percent hornblende, and 1 percent muscovite. Feldspar is partially sericitized. The granite also contains clots of minerals up to 2 mm in diameter, which include very fine-grained quartz, biotite, muscovite, and garnet(?), which are interpreted as xenoliths of metamorphic country rock, likely the Fortymile River assemblage. Xenoliths of andalusite-bearing phyllite and strongly foliated schist up to 10 cm were also reported by Jones and others (2017). Foliation was not observed in the granite. A U-Pb zircon age of 257 ± 2 Ma was reported by Jones and others (2017) from just north of the map area. Magnetic susceptibility of this unit is consistently low, 0.06–0.1 x 10^{-3} SI and averaging 0.08 x 10^{-3} SI.

METAMORPHIC ROCKS

Metamorphosed Ultramafic Rocks

TrPzum META-ULTRAMAFIC ROCKS (PALEOZOIC TO TRIASSIC?)—Multiple small bodies of metamorphosed ultramafic rock occurring as thrust-bound klippe above rocks of the parautochthonous Lake George assemblage. The small body in the west consists of predominantly fine- to medium-grained, partially-serpentinized meta-harzburgite and may include tectonic slivers of other ultramafic and mafic rock types. Outcrops are gray to black and weather orange-brown to white. The western body is 40–50 percent serpentine, 20–30 percent enstatite, 10–15 percent olivine, 5–10 percent diopside, 3–5 percent talc, and 3–5 percent chlorite, with about 2 percent magnetite. The two small bodies to the east are dark gray amphibole-bearing meta-harzburgite composed of 40–45 percent olivine, 6–30 percent

serpentine as alteration after olivine, 5–10 percent chlorite, up to 25 percent enstatite, 1–5 percent talc, up to 5 percent tremolite, up to 10 percent cummingtonite, 4–5 percent anthophyllite, up to 3 percent magnetite, minor residual diopside, and trace pyrrhotite. These minerals were confirmed by microprobe. Magnetic susceptibility is very high (8.2 to 24.6 x 10^{-3} SI, average 13.9 x 10^{-3} SI). The age of this unit is based on correlation with similar ultramafic rocks in the Mississippian to Upper Triassic Seventymile terrane, which has been mapped to the north in the Eagle Quadrangle (Foster and others, 1994), but correlation of rocks in the map area with the Seventymile terrane is still uncertain.

Metamorphic Rocks of the Yukon Tanana Terrane

Chicken Assemblage

Identified as the Chicken Metamorphic Complex by Werdon and others (2001), we herein refer to these fault-bound units as the Chicken assemblage to denote their shared metamorphic and tectonic history, which differs significantly from the nearby Fortymile River assemblage. In the map area the Chicken assemblage is dominated by metamorphosed arc-related mafic to intermediate volcanic rocks and subvolcanic dikes and sills. Fine- to medium-grained metasedimentary rocks are subordinate. In the Eagle A-2 Quadrangle, Werdon and others (2001) report similar rock types as well as andesitic to rhyolitic composition metavolcanic rocks that were not observed west of Taylor Mountain.

Mcms METASEDIMENTARY ROCKS UNDIVIDED (MISSISSIPPIAN)—The unit is composed of quartzite, muscovite-quartz schist, greenschist, marble and impure marble, and arkosic metasandstone. Quartzite and quartz schist are fine-grained, non-foliated to weakly foliated, and are commonly gray to tan. Foliation is defined by muscovite grains up to 2 mm long. Pale green to green-gray greenschist is composed of abundant quartz and lesser chlorite and muscovite. White to cream to beige marble layers are 10-meters- to more than 100-meters-thick, but are apparently not laterally continuous. It is unclear if the localized thickness of the marble units is a result of primary deposition or due to thickening and thinning during deformation. One marble layer near Gold Creek is heavily brecciated and hematite-stained. No fossils were observed in the marble units in the map area. Quartzite, quartz schist, and greenschist mineralogy includes 55–99 percent quartz, up to 15 percent chlorite, up to 15 percent muscovite, up to 15 percent albite, up to 5 percent epidote, up to 4 percent pyrite, and up to 3 percent calcite. Marble and impure marble mineralogy includes 80–100 percent calcite, up to 20 percent quartz, and trace hematite and kaolinite. Magnetic susceptibility is low to moderate (0.01–3.68 x 10^{-3} SI, average 0.54 x 10^{-3} SI). A detrital zircon U-Pb age sample from a quartzite near the mouth of Gold Creek has a maximum depositional age of 355 ± 7 Ma (21TJN105; Gavel and others, 2023), suggesting deposition in the Early Mississippian. This quartzite sample was interlayered with greenstone of unit Mcm, which also have Mississippian U-Pb zircon ages.

Mcm METAMAFIC ROCKS (MISSISSIPPIAN)—The unit is dominantly composed of non-foliated to weakly-foliated, fine-grained greenstones with basalt to basaltic andesite compositions interlayered with lesser fine- to coarse-grained metadiabase and metagabbro with similar compositions, as well as minor silicic metasedimentary layers. The unit is interpreted to represent a volcanic arc, with a mafic volcanic or hypabyssal protolith for the greenstone, and sills and/or dikes as protolith to the metagabbro. Contact relationships between metasedimentary rocks and greenstone are often parallel to foliation. Outcrops are commonly black or dark gray to green, weathering to brown or rusty orange. Mineralogy identified in thin section includes 30–60 percent hornblende, 30–60 percent plagioclase feldspar, 10–40 percent actinolite, 0–25 percent epidote, 0–15 percent chlorite, 0–10 percent clinozoisite, 0–10 percent quartz, 0–2 percent calcite, 0–3 percent magnetite, and 0–2 percent titanite. Rare calc-silicate hornfels

contains 30 percent hornblende, 15 percent feldspar, 20 percent epidote, and 35 percent diopside, with trace titanite and apatite. Primary igneous textures are common. Greenstone has up to 85 percent very fine-grained groundmass with up to 5-mm-long porphyritic plagioclase. Metagabbro has feldspar and amphibole porphyroclasts with grain sizes commonly between 0.5 and 5 mm and rarely up to 25 mm. Microprobe analyses of feldspars include both high-Ca plagioclase interpreted as relict igneous crystals or crystal cores and low-Ca albite grains interpreted to reflect greenschist facies metamorphism. Microprobe analyses of amphiboles include both primary igneous hornblende compositions and greenschist-facies metamorphic actinolite. Moderate anorthite composition plagioclase and metamorphic hornblende compositions were recorded on rims or as replacements of albite and actinolite, respectively, suggesting a late higher-temperature metamorphism, which is interpreted as hornblende-hornfels grade contact metamorphism, likely due to nearby plutons of the Taylor Mountain Plutonic suite. This widespread contact metamorphism and local observation of abundant Taylor Mountain suite dikes in the map area and in the adjacent Eagle A-2 quadrangle to the east (Werdon and others, 2001) suggest that Chicken assemblage contacts with the Taylor Mountain Batholith, Kechumstuk Mountain pluton and Diamond Mountain pluton are intrusive contacts. Magnetic susceptibility in the unit is variable (0.02–69.2 x 10^{-3} SI, average 9.0 x 10^{-3} SI, median 5.2 x 10^{-3} SI). Zircon from a metagabbro yielded a U-Pb age of 346.5 ± 5.5 Ma (Gavel and others, 2023) and a zircon U-Pb age of 344.0 ± 2.9 Ma was reported by Todd and others (2023) from a gabbroic sample, suggesting that the mafic protoliths in the Chicken assemblage are Early to Middle Mississippian.

Fortymile River Assemblage

The Fortymile River assemblage comprises a heterogeneous group of epidote amphibolite grade metamorphic lithologies, with interlayered metasedimentary rocks (quartzite, quartz schist, schist, marble, and paragneiss), amphibolite, and orthogneiss. Regionally, the age of this assemblage is constrained by datable interlayered lithologies. Orthogneiss, interpreted as having an igneous protolith, yield zircon U-Pb ages of ca. 355 to 341 Ma (Dusel-Bacon and others, 2006). Other felsic orthogneiss layers yield Permian zircon U-Pb ages and apparently represent later intrusions (Jones and others, 2017). A marble layer located northeast of the map area at the headwaters of Alder Creek in the Eagle B-2 Quadrangle yielded a mid-Mississippian to early Permian conodont age (Dusel-Bacon and Harris, 2003). This assemblage is a part of the Yukon–Tanana terrane as defined by Dusel-Bacon and others (2006) and is correlative to the Finlayson assemblages and possibly the Snowcap assemblage of Colpron and others (2006) in Canada. The Fortymile River assemblage is characterized by Triassic to Jurassic $^{40}Ar/^{39}Ar$ cooling ages (Dusel-Bacon and others, 2002; Jones and others, 2017; Naibert and others, 2018).

MDfo ORTHOGNEISS (DEVONIAN TO MISSISSIPPIAN)—Dominantly fine- to medium-grained orthogneiss of intermediate to felsic composition with subordinate interlayered metasedimentary rocks. The orthogneiss is typically pale gray to light brown, moderately foliated, has grain size of 0.01–15 mm. Gneissic textures are common and schistose textures are also observed. Petrography shows weak to moderate foliation is normally defined by biotite and lesser muscovite; S-C fabrics are common. Mineralogy consists of 40–75 percent plagioclase, 10–50 percent alkali feldspar, 5–50 percent quartz, 0–20 percent hornblende, 2–30 percent biotite, typically 1–3 percent, but up to 30 percent muscovite, and 5–15 percent chlorite (mostly as replacement of biotite and hornblende). Accessory minerals include garnet, epidote, hematite, magnetite, pyrite, and titanite. Magnetic susceptibility is generally low, 0.04–10.5 x 10^{-3} SI, averaging 0.18 x 10^{-3} SI. An orthogneiss in the northeast Tanacross quadrangle yielded a zircon U-Pb igneous crystallization age of 341.1 ± 2.3 Ma

and is correlative with this unit (Wypych and others, 2020).

MDfa AMPHIBOLITE (DEVONIAN TO MISSISSIPPIAN)—Fine- to medium-grained amphibolite and amphibole gneiss (both with partial to extensive greenschist facies overprint) interlayered with subordinate amphibole-bearing orthogneiss. The amphibolite is pale to dark green to gray-green, commonly with light white to gray bands, weathers brown, is foliated and commonly gneissic with rare schistose textures. Foliation is defined by aligned amphibole, biotite, and/or chlorite, the grain size is 0.1–3 mm with local hornblende porphyroblasts up to 30 mm. Mineralogy includes: 40–75 percent amphibole (dominantly hornblende, 0.1–2 mm, sometimes replaced by actinolite and chlorite), 15–50 percent plagioclase porphyroclasts (0.5–5 mm), 0–10 percent biotite (0.1–1 mm, can be partly altered to chlorite), 3–50 percent chlorite (includes both coarse euhedral and replacement, 0.1–2 mm), 0–20 percent garnet, and variable lesser amounts of epidote, magnetite, pyrite, and quartz. Magnetic susceptibility measurements vary widely: 0.04–36.6 x 10^{-3} SI, averaging 0.52 x 10^{-3} SI. The age is constrained by correlation with map unit MDfa in the Northeast Tanacross geologic map (Wypych and others, 2021), where a sample of amphibolite was dated by U-Pb zircon at 336.9 ± 3.8 Ma (Wypych and others, 2020).

MDfms METASEDIMENTARY ROCKS UNDIVIDED (DEVONIAN TO MISSISSIPPIAN)—Heterogeneous unit consisting of interlayered schist, quartz schist, quartzite, and paragneiss, with subordinate impure marble. Interlayered orthogneiss and amphibolite layers are not individually mappable within the unit. Minor marble or impure marble layers with white, yellow, gray, and bluish gray colors contain 35–95 percent calcite and 5–50 percent quartz. Marble layers range from cm to multiple meters thick and are most commonly associated with schistose layers. Metaconglomerate and graphitic quartzite layers are present locally. The unit also contains rare hornblende-bearing muscovite schist with radiating hornblende porphyroblasts up to 40 mm long along foliation planes, which are most often associated with amphibolite layers. Schist and quartz schist contain 3–40 percent muscovite, 0–30 percent biotite, 35–85 percent quartz, 5–30 percent feldspar, and 0–20 percent garnet. Garnet porphyroblasts are typically 1–3 mm in diameter and rarely up to 8 mm. Schistosity is defined by muscovite, variably chloritized biotite, and fine-grained quartz ribbons. Garnet porphyroblasts are commonly altered to biotite or chlorite along fractures and along grain edges. Feldspars are commonly altered to sericite. Paragneiss samples have similar mineralogy, with higher feldspar abundance (up to 50 percent) and less muscovite (5–25 percent). Gneissic banding is defined by quartz- and feldspar-rich layers separating quartz- and mica-rich layers. Quartzite contains 85–99 percent quartz, with 0.05–1 mm diameter anhedral crystals. Quartzite foliation is defined by elongate quartz grains and 1–10 percent micas, commonly muscovite and lesser biotite with minor chlorite replacement of biotite. Accessory minerals include epidote-clinozoisite, graphite, pyrite, and garnet. Magnetic susceptibility is 0.02–46.9 x 10^{-3} SI and averages 0.16 x 10^{-3} SI. Available U-Pb zircon ages from interlayered orthogneiss are 355–341 Ma (Dusel-Bacon and others, 2006; Wypych and others 2020), suggesting that sedimentation was Mississippian or older. Szumigala and others (2002b) and Werdon and others (2001) divide this unit into quartzite (pMq) and quartzite-paragneiss schist (pMqgs) units.

MDfmb MARBLE AND IMPURE MARBLE (DEVONIAN TO MISSISSIPPIAN)—White, yellow, pink, gray, or bluish-gray, medium- to very coarse-grained, non-fossiliferous crystalline calcite marble and quartz-calcite impure marble. The marble is locally dolomitic, has quartzose layers, and is sparsely micaceous (Flynn, 2003). Massive marble outcrops up to 10-m-thick commonly pinch and swell along strike and layers are sometimes discontinuous, likely due to folding or deformation. The unit locally contains clinopyroxene, epidote, garnet, quartz, and muscovite, as well as pyrite-bearing

quartz veins, thin pyrite bands, and/or disseminated pyrite. Magnetic susceptibility of this unit is very low, averaging 0.1 x 10^{-3} SI. This unit forms beds within metasedimentary and orthogneiss packages of Fortymile River assemblage. The unit is correlated with the marble and calcareous rocks unit (pMm) mapped in the Eagle A-1 and A-2 quadrangles (Szumigala and others, 2002b; Werdon and others, 2001) and the Finlayson assemblage marble unit (DMf5) in Yukon (Yukon Geological Survey, 2019). The age range of this unit is inferred from regional zircon data (Jones and others, 2017) and interlayered felsic metavolcanic rocks (orthogneiss) dated by U-Pb zircon methods (Day and others, 2002), although conodont evidence suggests the unit could be as young as early Early Permian (Dusel-Bacon and Harris, 2003).

Metamorphic Rocks of Parautochthonous North America

Jarvis Assemblage

The Jarvis assemblage, originally named the Jarvis belt by Dashevsky and others (2003), is composed of interlayered schistose metasedimentary rocks and felsic-dominant metavolcanic rocks. Metasediments include fine-grained metasandstones, siliceous mudstones, and local marble. Notably, massive to weakly foliated Triassic metagabbro bodies were intruded throughout the Jarvis assemblage and metamorphosed with the metavolcanic and metasedimentary rocks. These metagabbros are also present in parts of the Macomb belt, as defined by Dashevsky and others (2003), and we therefore include those parts of the Macomb belt with Triassic gabbros in our Jarvis assemblage. Jarvis assemblage rocks are distinguished from the Lake George assemblage by their younger depositional ages, which are inferred from the presence of interlayered Devonian-Mississippian metavolcanic rocks and a corresponding absence of Devonian-Mississippian metaplutonic rocks (Nokleberg and Aleinikoff, 1985; Twelker and others, 2021), along with the absence of Triassic metagabbro in the Lake George assemblage. The Jarvis assemblage is broadly characterized by greenschist-facies mineralogy (Dashevsky and others, 2003; Sicard and others, 2017), but relict hornblende and anorthite-rich plagioclase indicate these rocks reached amphibolite facies conditions prior to metamorphic cooling in the Early Cretaceous (Newberry and Twelker, 2021). These rocks are likely correlated with the White River complex in western Yukon (Ryan and others, 2013).

Trg METAGABBRO (TRIASSIC)—Fine-grained (0.1–3 mm), massive- to weakly foliated metagabbro to amphibolite of basaltic composition. Dark green to grayish-green. Mineralogy is dominated by a retrograde assemblage of actinolite, albite, and epidote-group minerals, with 40 to 70 percent amphiboles (hornblende and actinolite), 0–20 percent epidote, 0–30 percent clinozoisite, 0–20 percent albite, and minor titanite and muscovite. Microprobe examination of similar metagabbro in the Ladue River area reveals the presence of relict prograde metamorphic hornblende and plagioclase that locally retain cores of actinolite and albite, respectively, in addition to a retrograde overprint (Newberry and Twelker, 2021). The unit is therefore interpreted to have reached amphibolite facies metamorphism before greenschist facies retrograde metamorphism. Magnetic susceptibility ranges from 0.42–0.95 x 10^{-3} SI and averages 0.68 x 10^{-3} SI. Locally higher magnetic susceptibility values up to 70 x 10^{-3} SI were reported by Sicard and others (2017) in the adjacent Tok River area. A zircon sample from metagabbro yielded a U-Pb age of 228.9 ± 4.7 Ma (Gavel and others, 2023). The unit is correlated with the Snag Creek suite in Yukon (Ryan and others, 2013) and to Triassic metagabbro found in the eastern Alaska Range and southeastern Yukon Tanana Upland (Dashevsky and others, 2003; Sicard and others, 2017; Solie and others, 2019). Metagabbro appears to intrude as foliation parallel sills in the Jarvis assemblage and the White River Formation in adjacent parts of Yukon. Regionally, the sills range from sub-meter layers to irregular bodies more than 500 meters thick.

MDjq QUARTZITE AND QUARTZ SCHIST (DEVONIAN TO MISSISSIPPIAN)—Quartzite and quartz schist with minor calcareous schist, marble, and metafelsite. Based on the presence of interlayered amphibolite metagabbro sills, the unit is interpreted to have reached amphibolite facies metamorphic conditions before being partially retrograded to greenschist facies. The typical pale gray to tan quartz schist to quartzite contains 70–93 percent fine-grained (<0.2 mm) quartz forming about 1-mm-thick layers, with 0–10 percent feldspar. The siliceous layers are parted by about 0.2- to 0.5-mm-thick fine-grained muscovite (5–15 percent) and stilpnomelane (up to 10 percent) layers. Up to 10 percent of the muscovite is replaced by chlorite. Metamorphic chlorite composes about 5 percent of the rock. The micas commonly align in two directions and show S-C fabric. Rare calcite, graphite, and very small opaque specks are present. The unit typically displays a strong S1 foliation or cleavage orientation. Outcrop scale recumbent folds and similarly oriented axial planar cleavage define an F2 fabric and are well developed in more schistose units and interbedded marble. Magnetic susceptibility is generally low (averaging 0.63 x 10^{-3} SI). This unit is correlated to unit MDq of Sicard and others (2017). Zircon from a metafelsic layer in the Tok River area (15DR027) had a U-Pb age of 367.2 ± 2.8 Ma (Holm-Denoma and others, 2020). Richter (1975) has reported the presence of Middle Devonian corals in similar metamorphic rocks in the Nabesna Quadrangle.

Lake George Assemblage

The amphibolite-facies Lake George assemblage occupies the lowest structural level in the map area. The assemblage is composed of augen gneiss, orthogneiss, amphibolite, paragneiss, garnet-mica schist, quartz schist, and quartzite. The metasedimentary lithologies may be the metamorphosed equivalents of the Neoproterozoic–Devonian passive margin strata of the Selwyn Basin that were deposited prior to the intrusion of Mississippian-Devonian granitic plutons and sills. Orthogneiss and amphibolite form tabular bodies, which are usually concordant with foliation in the metasedimentary rocks. The rocks were metamorphosed to upper amphibolite facies (Newberry and Twelker, 2021) in the Early Cretaceous (Wildland, 2022) prior to rapidly cooling through the $^{40}Ar/^{39}Ar$ closure temperatures of multiple chronometers in the mid-Cretaceous (Pavlis and others, 1993; Dusel-Bacon and others, 2002; Jones and Benowitz, 2020; Naibert and others, 2020).

MDag DIVIDE MOUNTAIN AUGEN GNEISS (DEVONIAN TO MISSISSIPPIAN)—Homogeneous unit of deformed, locally mylonitic, and megacrystic orthogneiss with plutonic protoliths including granite and minor granodiorite. This unit is distinguished by its characteristic alkali-feldspar augen porphyroclasts, locally up to 80 mm long. These feldspars are commonly subhedral and often include sigma-type porphyroblasts showing the direction of shear. The unit is commonly white to light brown and has experienced varying degrees of weathering. Gneissic matrix is fine- to medium-grained, and mineralogy includes 25–45 percent subhedral to anhedral alkali feldspar, 15–20 percent anhedral plagioclase, 15–30 percent granoblastic quartz with irregular grain boundaries and common subgrains; 10–20 percent biotite; and 0–10 percent muscovite. Feldspars are commonly altered to sericite and biotite is variably altered to chlorite. The biotite and muscovite commonly form foliation-parallel, mm-scale bands which separate other felsic layers. Minor minerals include garnet, epidote, chlorite, oxides, and zircon. The unit is characteristically non-magnetic to weakly magnetic, with an average magnetic susceptibility of 0.19 x 10^{-3} SI. Twelker and others (2021) observed the transition from minimally strained megacrystic granite into mylonitic augen orthogneiss in the eastern Tanacross Quadrangle, with U-Pb zircon ages of 367.6 ± 8.4 and 360.7 ± 8.7 Ma respectively (samples 19SPR174 and 19ADW351C in Wildland and others, 2021). Todd and others (2019) obtained a U-Pb zircon age of 355.0 ± 4.5 Ma from augen orthogneiss in the Divide Mountain area

in the Tanacross D-1 Quadrangle. This augen gneiss unit correlates to the Divide Mountain Augen Gneiss of Wypych and others (2021) and Twelker and others (2021).

MDlo ORTHOGNEISS (DEVONIAN TO MISSISSIPPIAN)—Fine- to medium-grained, moderately foliated orthogneiss of intermediate to felsic composition occurring as tabular bodies interlayered with minor quartzite, paragneiss, amphibolite, and schist. This unit is locally mylonitic or schistose with a grain size of 0.1–10 mm; rare feldspar augen up to 20 mm. The unit is tan, light brown, and gray in color, minimally to partially weathered, and has experienced varying degrees of chlorite and sericite alteration. Mineralogy includes 15–50 percent anhedral to subhedral alkali feldspar, commonly twinned, inclusion-rich, and partially replaced by sericite, 15–50 percent subhedral plagioclase with polysynthetic twinning and sericite alteration, subhedral to anhedral dynamically recrystallized quartz (up to 10 percent in dioritic orthogneiss and up to 50 percent in granitic orthogneiss), up to 20 percent biotite with local chlorite replacement, up to 15 percent muscovite, and up to 10 percent hornblende. Biotite and muscovite commonly define the foliation. Hornblende is subhedral or occurs in amorphous clots with local chlorite alteration on grain boundaries. Accessory minerals include garnet, chlorite, pyrite, apatite, zircon, epidote, and titanite. The unit is generally non-magnetic with an average magnetic susceptibility of 0.85 x 10^{-3} SI. An orthogneiss from the map area yielded a U-Pb zircon crystallization age of 359.6 ± 1.3 Ma (sample 21SPR150; Gavel and others, 2023). A leucogranite orthogneiss yielded a U-Pb zircon crystallization age of 370.6 ± 8.3 Ma (sample 19ADW202; Wildland and others, 2021). This unit correlates to the Lake George orthogneiss of Twelker and others (2021) and Wypych and others (2021).

MDla AMPHIBOLITE (DEVONIAN TO MISSISSIPPIAN)—Amphibolite to amphibole-bearing gneiss commonly found interlayered with orthogneiss of unit MDlo. The unit is dark green to gray, commonly weathers to brown, is fine- to medium-grained, dominantly gneissic with lesser schistose textures. The predominant rock type is hornblende amphibolite (some partially retrograded to greenschist-facies) with 0.5–6mm grain size. Mineral composition includes 50–70 percent amphibole (subhedral, commonly with actinolite and tremolite cores and/or rims, some alteration to chlorite, 0.5–6 mm), 10–50 percent plagioclase (0.5–2 mm), 0–20 percent biotite (0.5–1 mm, typically with some alteration to chlorite), 0–10 percent chlorite (up to 40 percent in rare samples, includes both subhedral and replacement, 0.2–1 mm), and minor amounts of titanite, epidote, magnetite, garnet, and quartz. 1–2-mm-thick veins of quartz and lesser feldspar are common. Magnetic susceptibility is variable, 0.05–26 x 10^{-3} SI, averaging 1.5 x 10^{-3} SI. This amphibolite is correlated with Lake George assemblage amphibolite of Twelker and others (2021) and Wypych and others (2021) and unit pMa within the Alaska Highway Corridor (Solie and others, 2019). A U-Pb zircon age of 351.5 ± 4.3 Ma from correlative amphibolite was collected in the adjacent Northeast Tanacross area (Wypych and others, 2020).

pMlms METASEDIMENTARY ROCKS UNDIVIDED (PROTEROZOIC TO MISSISSIPPIAN)—A composite unit including quartzite, schist, quartz schist, and paragneiss and very rare impure marble. Quartzite is gray to pale green and weathers light tan to orange; very fine- to fine-grained (0.01–3 mm); weakly foliated; and are composed of 85–90 percent quartz (anhedral, sometimes parted by thin mica layers), 1–15 percent muscovite (fine-grained, often as single-crystal layers), 1–10 percent biotite, up to 5 percent feldspar (anhedral, locally stretched), and trace amounts of calcite, chlorite, pyrite, and garnet. Schist is pale gray, silver, silver-pink, or white weathering tan to orange with local iron staining. Schist and quartz schist are foliated, lineated, and often contain porphyroblastic garnet, with grain size of 0.1 to 10 mm. Felsic layers in the schist are composed of 20–70 percent quartz (0.5–2 mm, undulatory extinction, irregular grain boundaries, and forms thin sub-mm layers), 2–35 percent

feldspar (0.5–2 mm, twinned, forms bands, commonly replaced by sericite and is weathered), parted by sub-millimeter-thick mica layers containing 2–30 percent muscovite (fine-grained, found as individual grains and as inclusions in feldspar), 2–30 percent biotite (0.5–1mm, partially replaced by chlorite), and 0–10 percent euhedral garnet. Paragneiss is fine- to medium-grained. It contains less mica than schist and differs in texture—exhibiting gneissic banding and a generally finer grain size (0.1–4 mm). Metasedimentary lithologies of this unit have low magnetic susceptibility (0.01–5.7 x 10^{-3} SI, averaging about 0.37 x 10^{-3} SI). Orthogneiss within the metasediments suggests sediment deposition occurred prior to the Early Mississippian age of units MDag and MDlo. A detrital zircon sample along the Taylor Highway south of Taylor Mountain has a youngest U-Pb age population between 515 and 555 Ma (sample 16YTT021 in Jones and O'Sullivan, 2020), which suggests sediment is Cambrian or younger. The composite unit likely comprises the metamorphic equivalents of at least parts of the Neoproterozoic through Devonian Selwyn Basin stratigraphy. This unit is correlated to the Lake George metasedimentary rocks (pMlms) of Wypych and others (2021).

PMlp PARAGNEISS (PROTEROZOIC TO MISSISSIPPIAN)—Paragneiss interlayered with subordinate orthogneiss, quartzite, semischist, schist, and amphibolite. Paragneiss is predominantly black and white or tan to dark gray, weathering gray to brown. Paragneiss is foliated with gneissic and lesser schistose texture, with grain sizes of 0.1–6 mm; mineralogy includes: 40–80 percent quartz (0.2 to 2 mm, fine-grained, undulatory extinction, irregular grain boundaries, and forms thin sub-mm layers), 10–60 percent feldspar (0.5–2 mm, twinned, forms bands, some sericite replacement of alkali feldspar), 1–20 percent biotite (0.5–1 mm, well-aligned in foliation, typically fresh looking with some chlorite replacement, forms 1 mm thick layers), 1–10 percent muscovite (typically very fine-grained or found as inclusions in feldspar), and minor amounts of chlorite, garnet, sillimanite, andalusite, and/or iron oxide. Interlayered lithologies are of similar composition as those described for Lake George metasedimentary unit (pMlms). The unit is characterized by low magnetic susceptibility between 0.06 and 0.47 x 10^{-3} SI with a mean of 0.15 x 10^{-3} SI. Correlated with the Scottie Creek Formation in Canada (Yukon Geological Survey, 2019).

ACKNOWLEDGMENTS

We would like to thank Wes Buchanan for thorough and constructive reviews of the geologic maps, map unit descriptions, and report. We are grateful to have had access to Doyon Limited lands within the study area. The DGGS Western Tanacross project was jointly funded by the U.S. Geological Survey's Earth Mapping Resources Initiative (Earth MRI) program through cooperative agreement G20AC00156 and the State of Alaska. The DGGS Taylor Mountain project was jointly funded by the U.S. Geological Survey's Earth MRI program through cooperative agreement G21AC00336 and the State of Alaska. The views and conclusions contained in this document are those of the authors and should not be interpreted as representing the opinions or policies of the U.S. Geological Survey. Mention of trade names or commercial products does not constitute their endorsement by the U.S. Geological Survey.

Table 1. Geochronology samples in the Western Tanacross and Taylor Mountain project areas.

Age Type	Sample ID	Age (Ma)	2σ Age Error (Ma)	Notes	Reference	Latitude (NAD83)	Longitude (NAD83)
Biotite $^{40}Ar/^{39}Ar$	21AKH129	110.84	0.09	Plateau age; cooling age	Naibert and others, 2023	63.9001	-143.7901
Biotite $^{40}Ar/^{39}Ar$	21RN239	111.8	4.8	Plateau age; skarn formation age	Gavel and others, 2023	63.2670	-143.3987
Biotite $^{40}Ar/^{39}Ar$	21RN530	100.83	0.51	Plateau age; crystallization age	Naibert and others, 2023	63.7676	-142.1378
Hornblende $^{40}Ar/^{39}Ar$	21ADW058	176.15	1.08	Weighted mean age; cooling age	Naibert and others, 2023	63.9178	-143.3539
Hornblende $^{40}Ar/^{39}Ar$	21ET207	192.90	2.02	Plateau age; cooling age	Naibert and others, 2023	63.8602	-142.5884
Muscovite $^{40}Ar/^{39}Ar$	21ADW241	109.56	0.37	Weighted mean age; cooling age	Naibert and others, 2023	63.8620	-142.1500
Muscovite $^{40}Ar/^{39}Ar$	21ADW289	130.59	1.37	Weighted mean age; cooling age	Naibert and others, 2023	63.9310	-141.7643
Muscovite $^{40}Ar/^{39}Ar$	21AKH040	112.34	0.17	Weighted mean age; cooling age	Naibert and others, 2023	63.8865	-143.3964
Muscovite $^{40}Ar/^{39}Ar$	21AKH111	130.21	1.03	Weighted mean age; cooling age	Naibert and others, 2023	63.2813	-143.8163
Muscovite $^{40}Ar/^{39}Ar$	21AW088	119.97	0.30	Weighted mean age; cooling age	Naibert and others, 2023	63.2813	-143.8019
Muscovite $^{40}Ar/^{39}Ar$	21ET169	114.21	0.44	Weighted mean age; vein formation age	Naibert and others, 2023	63.2607	-143.8084
Muscovite $^{40}Ar/^{39}Ar$	21ET179	120.27	0.93	Weighted mean age; vein formation age	Naibert and others, 2023	63.2824	-143.8397
Muscovite $^{40}Ar/^{39}Ar$	21MLB046	120.90	0.59	Weighted mean age; cooling age	Naibert and others, 2023	63.7053	-143.3158
Muscovite $^{40}Ar/^{39}Ar$	21RN612	85.63	0.23	Integrated age; low confidence skarn formation age	Naibert and others, 2023	64.2558	-142.7118
Muscovite $^{40}Ar/^{39}Ar$	21TJN154	103.44	0.41	Weighted mean age; cooling age	Naibert and others, 2023	63.9586	-141.7854
Muscovite $^{40}Ar/^{39}Ar$	21TJN257	115.42	0.81	Weighted mean age; cooling age	Naibert and others, 2023	63.8789	-142.0384
Sericite $^{40}Ar/^{39}Ar$	21ET242	191.39	1.12	Plateau age; vein formation age	Naibert and others, 2023	64.0992	-142.0382
Sericite $^{40}Ar/^{39}Ar$	21ET252	190.70	2.64	Weighted mean; vein formation age	Naibert and others, 2023	64.1089	-142.3460
Detrital Zircon U-Pb	16YTT021			Sample collected for detrital zircon; MDA of 515-555 Ma	Jones and O'Sullivan, 2020	63.9082	-141.7709
Detrital Zircon U-Pb	17AJJ128			Sample collected for detrital zircon	Jones and O'Sullivan, 2020	64.2395	-142.5630
Detrital Zircon U-Pb	18ET413			Sample collected for detrital zircon; YSP MDA of 105.4 +/- 5.6 Ma	Wypych and others, 2020	63.8795	-141.6491
Detrital Zircon U-Pb	21ADW211			Sample collected for detrital zircon; YSP MDA of 250.6 +/- 5.2 Ma	Gavel and others, 2023	63.9651	-141.7839
Detrital Zircon U-Pb	21AW047			Sample collected for detrital zircon; YSP MDA of 375.0 +/- 7.8 Ma	Gavel and others, 2023	63.7087	-143.1939
Detrital Zircon U-Pb	21DFA125			Sample collected for detrital zircon; YSP MDA of 417.8 +/- 9.1 Ma	Gavel and others, 2023	64.2479	-142.1527

Table 1, cont. Geochronology samples in the Western Tanacross and Taylor Mountain project areas.

Age Type	Sample ID	Age (Ma)	2σ Age Error (Ma)	Notes	Reference	Latitude (NAD83)	Longitude (NAD83)
Detrital Zircon U-Pb	21ET094			Sample collected for detrital zircon; YSP MDA of 70.0 +/- 1.4 Ma	Gavel and others, 2023	63.4382	-142.5626
Detrital Zircon U-Pb	21ET192			Sample collected for detrital zircon; YSP MDA of 67.4 +/- 1.4 Ma.	Gavel and others, 2023	63.6507	-143.5258
Detrital Zircon U-Pb	21RN401			Sample collected for detrital zircon; YSP MDA of 68.8 +/- 1.4 Ma	Gavel and others, 2023	63.8526	-142.3778
Detrital Zircon U-Pb	21TJN105			Sample collected for detrital zircon; YSP MDA of 355.2 +/- 7.2 Ma	Gavel and others, 2023	64.1091	-142.3450
Zircon U-Pb	13ATe010	212.5	3.0	Crystallization age	Todd and others, 2023	63.9861	-142.1445
Zircon U-Pb	14AJJ002	365.5	4.5	Crystallization age	Jones and O'Sullivan, 2020	63.8177	-142.6035
Zircon U-Pb	14AJJ048A	363.4	5.9	Crystallization age; rims/exteriors suggest ca. 113 Ma overgrowth	Jones and O'Sullivan, 2020	63.7991	-142.6891
Zircon U-Pb	14AJJ048C	360.3	6.6	Crystallization age; rims/exteriors suggest ca. 111 Ma overgrowth	Jones and O'Sullivan, 2020	63.7991	-142.6891
Zircon U-Pb	14ATe108A	111.7	0.6	Crystallization age	Todd and others, 2023	63.6339	-142.7755
Zircon U-Pb	14ATe120E	184.0	1.2	Crystallization age	Todd and others, 2023	64.1365	-142.4691
Zircon U-Pb	15AJJ105C	349.7	3.8	Crystallization age; few Permian ages on bright overgrowths	Jones and O'Sullivan, 2020	63.7692	-142.7636
Zircon U-Pb	15ATe110A	198.8	1.0	Crystallization age	Todd and others, 2023	64.1325	-142.6209
Zircon U-Pb	15ATe110B	204.9	1.2	Crystallization age	Todd and others, 2023	64.1327	-142.6211
Zircon U-Pb	15ATe126A	214.1	1.8	Crystallization age	Todd and others, 2023	64.0463	-142.8342
Zircon U-Pb	15ATe127A	207.3	2.0	Crystallization age	Todd and others, 2023	64.1492	-142.7641
Zircon U-Pb	15ATe129A	210.6	1.8	Crystallization age	Todd and others, 2023	64.0484	-142.2736
Zircon U-Pb	15ATe203	205.1	4.1	Crystallization age	Todd and others, 2023	64.0643	-142.0052
Zircon U-Pb	16AJJ001	204.6	3.6	Crystallization age	Jones and O'Sullivan, 2020	63.8931	-142.2335
Zircon U-Pb	16AJJ003	214.6	1.8	Crystallization age	Todd and others, 2023	64.0257	-142.3147
Zircon U-Pb	16ATe123C	205.5	1.7	Crystallization age	Todd and others, 2023	63.8938	-142.2328
Zircon U-Pb	16ATe133A	200.1	2.8	Crystallization age	Todd and others, 2023	64.2417	-142.1999
Zircon U-Pb	16ATe134A	208.5	1.7	Crystallization age	Todd and others, 2023	64.1358	-142.5023
Zircon U-Pb	16ATe134C	344.0	2.9	Crystallization age	Todd and others, 2023	64.1355	-142.4757
Zircon U-Pb	16YTT020A	360.1	7.3	Crystallization age	Jones and O'Sullivan, 2020	63.8981	-141.7700

Table 1, cont. Geochronology samples in the Western Tanacross and Taylor Mountain project areas.

Age Type	Sample ID	Age (Ma)	2σ Age Error (Ma)	Notes	Reference	Latitude (NAD83)	Longitude (NAD83)
Zircon U-Pb	17ADk227	101.2	0.8	Crystallization age	Todd and others, 2023	63.8864	-143.4613
Zircon U-Pb	17AJJ125	359.3	8.4	Crystallization age	Jones and O'Sullivan, 2020	64.2479	-142.5509
Zircon U-Pb	17AJJ127	363.5	3.0	Crystallization age	Todd and others, 2023	64.2441	-142.5662
Zircon U-Pb	17AJJ127	373.2	4.6	Crystallization age	Jones and O'Sullivan, 2020	64.2440	-142.5662
Zircon U-Pb	18ADK104	69.8	0.7	Crystallization age	Todd and others, 2023	63.8915	-143.4667
Zircon U-Pb	18ADK105A	100.4	0.9	Crystallization age	Todd and others, 2023	63.9814	-143.2945
Zircon U-Pb	18AJJ033	186.5	2.9	Crystallization age	Jones and O'Sullivan, 2020	63.8412	-143.3279
Zircon U-Pb	18AJJ035B	258.1	2.5	Crystallization age	Jones and O'Sullivan, 2020	63.9742	-141.7307
Zircon U-Pb	18AJJ035B	259.5	3.2	Crystallization age	Todd and others, 2023	63.9743	-141.7307
Zircon U-Pb	19AJJ006B	208.2	3.8	Crystallization age	Jones and O'Sullivan, 2020	63.9126	-143.3340
Zircon U-Pb	19ATe003A	69.6	0.5	Crystallization age	Todd and others, 2023	63.8080	-141.6803
Zircon U-Pb	19ATe005A	201.4	1.5	Crystallization age	Todd and others, 2023	64.1343	-142.5650
Zircon U-Pb	19ATe009A	212.2	1.4	Crystallization age	Todd and others, 2023	64.0490	-142.3006
Zircon U-Pb	19ATe009B	204.7	2.5	Crystallization age	Todd and others, 2023	64.0490	-142.3006
Zircon U-Pb	19ATe009C	213.2	4.8	Crystallization age	Todd and others, 2023	64.0490	-142.3006
Zircon U-Pb	19ATe020A	208.1	1.8	Crystallization age	Todd and others, 2023	63.9949	-142.3534
Zircon U-Pb	20ADW001	108.4	2.2	Crystallization age	Gavel and others, 2023	63.5541	-143.0607
Zircon U-Pb	21ADW052	186.8	3.8	Crystallization age; few zircon	Gavel and others, 2023	63.8866	-143.3805
Zircon U-Pb	21ADW136	202.2	4.1	Crystallization age	Gavel and others, 2023	63.8924	-142.2641
Zircon U-Pb	21ADW146	215.6	4.4	Crystallization age	Gavel and others, 2023	63.9698	-142.9289
Zircon U-Pb	21AW088			No age due to strong alteration and Pb loss. Some concordant Proterozoic grains.	Gavel and others, 2023	63.2813	-143.8019
Zircon U-Pb	21AW108	268.1	5.4	Crystallization age	Gavel and others, 2023	63.3295	-143.9443
Zircon U-Pb	21AW136	185.4	3.7	Crystallization age	Gavel and others, 2023	63.9310	-143.0696
Zircon U-Pb	21AW152	201.0	4.0	Crystallization age	Gavel and others, 2023	63.8893	-142.0292
Zircon U-Pb	21AW180	191.1	3.8	Crystallization age	Gavel and others, 2023	64.0143	-142.3274
Zircon U-Pb	21AW185	203.3	4.1	Crystallization age	Gavel and others, 2023	64.0094	-142.2493

Table 1, cont. Geochronology samples in the Western Tanacross and Taylor Mountain project areas.

Age Type	Sample ID	Age (Ma)	2σ Age Error (Ma)	Notes	Reference	Latitude (NAD83)	Longitude (NAD83)
Zircon U-Pb	21AW196			No age due to strong alteration and Pb loss. Some concordant Proterozoic grains.	Gavel and others, 2023	64.2467	-142.1625
Zircon U-Pb	21DFA047	68.3	1.4	Crystallization age	Gavel and others, 2023	64.0129	-142.9112
Zircon U-Pb	21ET101	275.5	5.6	Crystallization age	Gavel and others, 2023	63.4281	-142.6028
Zircon U-Pb	21ET119	110.8	2.2	Crystallization age	Gavel and others, 2023	63.6841	-143.5388
Zircon U-Pb	21ET193	110.0	2.2	Crystallization age	Gavel and others, 2023	63.6469	-143.5675
Zircon U-Pb	21ET227	184.8	3.7	Crystallization age	Gavel and others, 2023	63.9895	-143.1243
Zircon U-Pb	21ET257	56.2	1.1	Crystallization age	Gavel and others, 2023	64.1744	-142.2281
Zircon U-Pb	21MLB006	108.7	2.2	Crystallization age	Gavel and others, 2023	63.5810	-142.5531
Zircon U-Pb	21MLB187	183.8	3.7	Crystallization age	Gavel and others, 2023	63.9893	-143.1247
Zircon U-Pb	21MLB248	56.9	1.1	Crystallization age	Gavel and others, 2023	64.2227	-142.5086
Zircon U-Pb	21MMG105	1429	28.4	Inheritance age	Gavel and others, 2023	64.1831	-142.0937
Zircon U-Pb	21MMG119	346.5	7.0	Crystallization age	Gavel and others, 2023	64.1283	-142.3721
Zircon U-Pb	21MMG201	266.8	5.4	Crystallization age	Gavel and others, 2023	64.0455	-142.5333
Zircon U-Pb	21RN094	109.8	2.2	Crystallization age	Gavel and others, 2023	63.5450	-143.2709
Zircon U-Pb	21RN257	228.9	4.7	Crystallization age	Gavel and others, 2023	63.3110	-143.9736
Zircon U-Pb	21RN282	107.2	2.2	Crystallization age	Gavel and others, 2023	63.4329	-142.6031
Zircon U-Pb	21RN399			No age due to strong alteration, poor zircon yield, and Pb loss. Two concordant Cretaceous grains.	Gavel and others, 2023	63.8602	-142.3739
Zircon U-Pb	21SPR026	108.4	2.2	Crystallization age	Gavel and others, 2023	63.5418	-142.7602
Zircon U-Pb	21SPR068	360.7	1.7	Crystallization age	Gavel and others, 2023	63.7187	-143.2511
Zircon U-Pb	21SPR150	359.6	1.3	Crystallization age	Gavel and others, 2023	63.8771	-143.8071
Zircon U-Pb	21TJN008	110.4	2.2	Crystallization age	Gavel and others, 2023	63.8460	-143.8462
Zircon U-Pb	21TJN101	204.4	4.1	Crystallization age	Gavel and others, 2023	64.0992	-142.0385
Zircon U-Pb	21TJN114			No age due to strong alteration, poor zircon yield, and Pb loss. Two concordant Cretaceous grains.	Gavel and others, 2023	64.1961	-142.1443
Zircon U-Pb	21TJN161	211.3	4.2	Crystallization age	Gavel and others, 2023	63.9689	-141.9156

Table 1, cont. Geochronology samples in the Western Tanacross and Taylor Mountain project areas.

Age Type	Sample ID	Age (Ma)	2σ Age Error (Ma)	Notes	Reference	Latitude (NAD83)	Longitude (NAD83)
Zircon U-Pb	21TJN180	107.6	2.2	Crystallization age	Gavel and others, 2023	63.8860	-142.6639
Zircon U-Pb	21TJN226	352.0	4.1	Crystallization age	Gavel and others, 2023	64.2482	-142.6939
Zircon U-Pb	21TJN234	203.4	1.4	Crystallization age	Gavel and others, 2023	64.1834	-142.5240
Zircon U-Pb	21TJN264	70.1	1.4	Crystallization age	Gavel and others, 2023	64.1309	-142.2785
Zircon U-Pb	21WCW008	71.1	1.4	Crystallization age	Gavel and others, 2023	63.8351	-143.9774
Zircon U-Pb	22IPM013	189.3	3.2	Crystallization age	Gavel and others, in press	64.1779	-142.4302
Zircon U-Pb	22TJN033	66.8	3.6	Crystallization age	Gavel and others, in press	63.8524	-142.3325
Zircon U-Pb	80714 2A	374.1	3.7	Crystallization age	Todd and others, 2023	63.7287	-142.8612

REFERENCES

Allan, M.M., Mortensen, J.K., Hart, C.R, Bailey, L.A., Sanchez, M.G., Ciolkiewicz, Wiltold, McKenzie, G.G., and Creaser, R.A., 2013, Magmatic and metallogenic framework of west-central Yukon and eastern Alaska, *in* Colpron, Maurice, Bissig, Thomas, Rusk, B.G., and Thompson, J.F.H., Tectonics, Metallogeny, and Discovery: The North American Cordillera and Similar Accretionary Settings, Society of Economic Geologists, Special Publication 17, p. 111–168.

Bacon, C.R., Dusel-Bacon, Cynthia, Aleinikoff, J.N., and Slack, J.F., 2014, The Late Cretaceous Middle Fork Caldera, its resurgent intrusion, and enduring landscape stability in east-central Alaska: Geosphere, v. 10, no. 6, p. 1432–1455. https://doi.org/10.1130/GES01037.1

Bacon, C.R., Foster, H.L., and Smith, J.G., 1990, Rhyolitic calderas of the Yukon–Tanana terrane, east-central Alaska— Volcanic remnants of a mid-Cretaceous magmatic arc: Journal of Geophysical Research, v. 95, no. B13, p. 21,451–21,461. http://doi.org/10.1029/JB095iB13p21451

Barker, Fred, 1979, Chapter 1-Trondhjemite: Definition, Environment, and Hypotheses on Origin, Developments in Petrology, v. 6, p. 1–12.

Beranek, L.P., and Mortensen, J.K., 2011, The timing and provenance record of the Late Permian Klondike orogeny in northwestern Canada and arc-continent collision along western North America, Tectonics, v. 30, TC5017.

Blondes, M.S., Reiners, P.W., Edwards, B.R., and Biscontini, Adrian, 2007, Dating young basalt eruptions by (U-Th)/He on xenolithic zircons: Geology, v. 35, no. 1, p. 17–20. https://doi.org/10.1130/G22956A.1

Burns, L.E., Barefoot, J.D., Graham, G.R.C., Fugro Airborne Surveys Corp., and Stevens Exploration Management Corp., 2019, Western Fortymile electromagnetic and magnetic airborne geophysical survey data compilation: Alaska Division of Geological & Geophysical Surveys Geophysical Report 2019-7, 12 p. https://doi.org/10.14509/30178

Burns, L.E., Geoterrex-Dighem, Stevens Exploration Management Corp., Emond, A.M., and Graham, G.R.C., 2015, Fortymile mining district electromagnetic and magnetic airborne geophysical survey data compilation: Alaska Division of Geological & Geophysical Surveys Geophysical Report 2015-4, 12 p. https://doi.org/10.14509/29411

Colpron, Maurice, 2001, Geochemical characterization of Carboniferous volcanic successions from Yukon–Tanana Terrane, Glenlyon map area (105L), central Yukon, *in* Emond, D.S., and Weston, L.H., eds., Yukon exploration and geology, 2000, Exploration and Geological Services Division, Indian and Northern Affairs Canada, p. 111–136.

Colpron, Maurice, Murphy, D.C., Skipton, Diane, 2023, the Late Triassic Galena and Snag Creek sills, Yukon: Age, Geochemistry, and Correlations (poster), Cordilleran Tectonic Workshop 2023 program and abstracts, Whitehorse, Yukon, March 3–5, 2023.

Colpron, Maurice, Nelson, J.L., and Murphy, D.C., 2006, A tectonostratigraphic framework for the pericratonic terranes of the northern Canadian Cordillera, *in* Colpron, Maurice, and Nelson, J.L., eds., Paleozoic evolution and metallogeny of pericratonic terranes at the ancient Pacific margin of North America, Canadian and Alaskan Cordillera: Geological Association of Canada Special Paper, v. 45, p. 1–23.

Dashevsky, S.S., Schaefer, C.F., and Hunter, E.N., 2003, Bedrock geologic map of the Delta mineral belt, Tok mining district, Alaska: Alaska Division of Geological & Geophysical Surveys Professional Report 122, 122 p., 2 sheets, scale 1:63,360. https://doi.org/10.14509/2923

Day, W.C., Aleinikoff, J.N., and Gamble, B.M., 2002, Geochemistry and age constraints on metamorphism and deformation in the Fortymile River area, eastern Yukon-Tanana Upland, Alaska, *in* Wilson, F.H., and Galloway, J.P., eds., Studies by the U.S. Geological Survey in Alaska, 2000: U.S. Geological Survey Professional Paper 1662, p. 5–18.

Day, W.C., O'Neill, J.M., Aleinikoff, J.N., Green, G.N., Saltus, R.W., and Gough, L.P., 2007, Geologic map of

the Big Delta B-1 Quadrangle, east-central Alaska: U.S. Geological Survey Scientific Investigations Map 2975, 1 sheet, scale 1:63,360.

Day, W.C., O'Neill, J.M., Dusel-Bacon, Cynthia, Aleinikoff, J.N., and Siron, C.R., 2014, Geologic map of the Kechumstuk fault zone in the Mount Veta area, Fortymile mining district, east-central Alaska: U.S. Geological Survey Scientific Investigations Map 3291, 1 sheet, scale 1:63,360.

Dusel-Bacon, Cynthia, Aleinikoff, J.N., Day, W.C., and Mortensen, J.K., 2015, Mesozoic magmatism and timing of epigenetic Pb-Zn-Ag mineralization in the western Fortymile mining district, east-central Alaska: Zircon U-Pb geochronology, whole-rock geochemistry, and Pb isotopes: Geosphere, v. 11, no. 3, p. 786–822.

Dusel-Bacon, Cynthia, Bacon, C.R., O'Sullivan, P.B., Day, W.C., 2016, Apatite fission-track evidence for regional exhumation in the subtropical Eocene, block faulting, and localized fluid flow in east-central Alaska. Canadian Journal of Earth Sciences, v. 53, p. 260–280.

Dusel-Bacon, Cynthia, and Harris, A.G., 2003, New occurrences of late Paleozoic and Triassic fossils from the Seventymile and Yukon-Tanana Terranes, east-central Alaska, with comments on previously published occurrences in the same area: Studies by the U.S. Geological Survey in Alaska, 2001: U.S. Geological Survey Professional Paper 1678, p. 5–30.

Dusel-Bacon, Cynthia, Hopkins, M.J., Mortensen, J.K., Dashevsky, S.S., Bressler, J.R., and Day, W.C., 2006, Paleozoic tectonic and metallogenic evolution of the pericratonic rocks of east-central Alaska and adjacent Yukon, *in* Colpron, Maurice and Nelson J.L., eds., Paleozoic Evolution and Metallogeny of Pericratonic Terranes at the Ancient Pacific Margin of North America, Canadian and Alaskan Cordillera: Geological Association of Canada Special Paper 45, p. 25–74.

Dusel-Bacon, Cynthia, Lanphere, M.A., Sharp, W.D., Layer, P.W., and Hansen, V.L., 2002, Mesozoic thermal history and timing of structural events for the Yukon-Tanana Upland, east-central Alaska: $^{40}Ar/^{39}Ar$ data from metamorphic and plutonic rocks: Canadian Journal of Earth Sciences, v. 39, no. 6, p. 1,013–1,051. doi.org/10.1139/e02-018

Dusel-Bacon, Cynthia, Slack, J.F., Aleinikoff, J.N., and Mortensen, J.K., 2009, Mesozoic magmatism and base-metal mineralization in the Fortymile mining district, eastern Alaska—Initial results of petrographic, geochemical, and isotopic studies in the Mount Veta area, *in* Haeussler, P.J., and Galloway, J.P., Studies by the U.S. Geological Survey in Alaska, 2007: U.S. Geological Survey Professional Paper 1760–A, 42 p. http://pubs.usgs.gov/pp/1760/a/

Emond, A.M., and MPX Geophysics LTD, 2021, Eagle airborne magnetic and radiometric geophysical survey: Alaska Division of Geological & Geophysical Surveys Geophysical Report 2021-2, 4 p. https://doi.org/10.14509/30755

Emond, A.M., Saltus, R.W., Graham, G.R.C., and Goldak Airborne Surveys, 2015, Airborne magnetic geophysical survey of the Tanacross region, Alaska: Alaska Division of Geological & Geophysical Surveys Geophysical Report 2015-6, 12 p. https://doi.org/10.14509/29514

Flynn, R.L., 2003, Geology of the Boundary area, Eagle A-1 and Tanacross D-1 quadrangles, east-central Alaska: Fairbanks, Alaska, University of Alaska Fairbanks, M.S. thesis, 185 p.

Foster, H.L., 1967, Geology of the Mount Fairplay area, Alaska: U.S. Geological Survey Bulletin 1241-B, p. B1-B18, 1 sheet, scale 1:63,360.

———1970, Reconnaissance geologic map of the Tanacross Quadrangle, Alaska: U.S. Geological Survey Miscellaneous Geologic Investigations Map 593, 1 sheet, scale 1:250,000.

Foster, H.L., comp., 1976, Geologic map of the Eagle Quadrangle, Alaska: U.S. Geological Survey Miscellaneous Investigations Series Map 922, 1 sheet, scale 1:250,000.

Foster, H.L., and Igarashi, Yaeko, 1990, Fossil pollen from nonmarine sedimentary rocks of the eastern Yukon-Tanana region, east-central Alaska, *in* Dover, J.H., and Galloway, J.P., eds., Geologic studies in Alaska by the U.S. Geological Survey, 1989: U.S. Geological Survey Bulletin 1946, p. 11–20.

Foster, H.L., Keith, T.E.C., and Menzie, W.D., 1994, Geology of the Yukon-Tanana area of east-central Alaska, *in* Plafker, George, and Berg, H.C., eds., The Geology of Alaska: Geological Society of America, p. 205–240.

Gavel, M.M., Regan, S.P., Holland, Mark, Wildland, A.D., Wypych, Alicja, Naibert, T.J., and Twelker, Evan, 2023, U-Pb zircon geochronology of bedrock samples collected in the Eagle and Tanacross quadrangles, eastern Alaska: Alaska Division of Geological & Geophysical Surveys Preliminary Interpretive Report 2023-2, 38 p. https://doi.org/10.14509/31013

Gavel, M.M., Wildland, A.D., Fessenden, S.N., Naibert, T.J., Twelker, Evan, Wypych, Alicja, and O'Sullivan, P.B., in press, Uranium lead ages and isotope ratios of igneous and metamorphic zircon from the Mount Harper project area: Alaska Division of Geological & Geophysical Surveys Raw Data File 2024-2, 6 p. https://doi.org/10.14509/31123

Hammarstrom, J.H., and Dicken, C.L., 2019, Focus areas for data acquisition for potential domestic sources of critical minerals—Rare earth elements (ver. 1.1, July 2022), chap. A of U.S. Geological Survey, Focus areas for data acquisition for potential domestic sources of critical minerals: U.S. Geological Survey Open-File Report 2019–1023, 11 p.

Hansen, V.L., and Dusel-Bacon, Cynthia, 1998, Structural and kinematic evolution of the Yukon-Tanana Upland tectonites, east-central Alaska—A record of late Paleozoic to Mesozoic crustal assembly: Geological Society of America Bulletin v. 110, no. 2, p. 211–230.

Hansen, V.L., Heizler, M.T., and Harrison, T.M., 1991, Mesozoic thermal evolution of the Yukon-Tanana composite terrane; new evidence from $^{40}Ar/^{39}Ar$ data: Tectonics, v. 10, no. 1, p. 51–76.

Holm-Denoma, C.S., Sicard, K.R., and Twelker, Evan, 2020, U-Pb geochronology of igneous and detrital zircon samples from the Tok River area, eastern Alaska Range, and Talkeetna Mountains, Alaska: Alaska Division of Geological & Geophysical Surveys Raw Data File 2020-3, 20 p. https://doi.org/10.14509/30439

Jones, J.V., III, and Benowitz, J.A., 2020, $^{40}Ar/^{39}Ar$ isotopic data and ages for rocks from the Yukon-Tanana upland of eastern Alaska and the northern Aleutian Range of south-central Alaska: U.S. Geological Survey Data Release. https://doi.org/10.5066/P96762V3

Jones, J.V., III, and O'Sullivan, Paul, 2020, U-Pb isotopic data and ages of zircon, titanite, and detrital zircon from rocks from the Yukon-Tanana Upland, Alaska: U.S. Geological Survey Data Release. https://doi.org/10.5066/P9WWV93S

Jones, J.V., III, Todd, Erin, Caine, J.S., Holm-Denoma, C.S., Ryan, J.J., and Benowitz, J.A., 2017, Late Permian (ca. 267–257 Ma) magmatism, deformation, and metamorphism and lithotectonic associations of the Ladue River unit in east-central Alaska [abs.]: Geological Society of America Abstracts with Programs, v. 49, no. 6. https://doi.org/10.1130/abs/2017AM-304170

Knight, Eleanor, Schneider, D.A., and Ryan, J.J., 2013, Thermochronology of the Yukon-Tanana Terrane, West-Central Yukon: Evidence for Jurassic Extension and Exhumation in the Northern Canadian Cordillera: the Journal of Geology, v. 121, p. 371–400.

Kreiner, D.C., and Jones, J.V., III, 2020, Focus areas for data acquisition for potential domestic resources of 11 critical minerals in Alaska—Aluminum, cobalt, graphite, lithium, niobium, platinum group elements, rare earth elements, tantalum, tin, titanium, and tungsten (ver. 1.1, July 2022), Chapter C of U.S. Geological Survey, Focus areas for data acquisition for potential domestic sources of critical minerals: U.S. Geological Survey Open-File Report 2019-1023, 20 p.

Kreiner, D.C., Jones, J.V., III, and Case, G.N., 2022, Alaska focus area definition for data acquisition for potential domestic sources of critical minerals in Alaska for antimony, barite, beryllium, chromium, fluorspar, hafnium, magnesium, manganese, uranium, vanadium, and zirconium, Chapter E of U.S. Geological Survey, Focus areas for data acquisition for potential domestic sources of critical minerals: U.S. Geological Survey Open-File Report 2019-1023, 19 p.

Lowey, G.V., and Hills, L.V., 1988, Lithofacies, petrography and environments of deposition, Tantalus Formation (Lower Cretaceous) Indian River area, West-Central Yukon: Bulletin of Canadian Petroleum Geology, v. 36, p. 296–310.

Mair, J.L., Hart, C.J.R., Stephens, J.R., 2006, Deformation history of the northwestern Selwyn Basin, Yukon, Canada: Implications for orogen evolution and mid-Cretaceous magmatism: Geological Society of America Bulletin, v. 118, p. 304–323.

Mertie, J.B., Jr., 1931, A geologic reconnaissance of the Dennison Fork district, Alaska: U.S. Geological Survey Bulletin 827, 44 p., 2 sheets, scale 1:250,000.

Moynihan, David, and Crowley, J.L., 2022, Preliminary observations on the geology of the southern Big Salmon Range, south-central Yukon (parts of NTS 105C/13,14, 105F/4 and 105E/1), *in* MacFarlane, K.E., Yukon Exploration and Geology 2021: Yukon Geological Survey, p. 217–265.

Murphy, D.C., Mortensen, J.K., Piercey, S.J., Orchard, M.J. and Gehrels, G.E., 2006, Mid-Paleozoic to early Mesozoic tectonostratigraphic evolution of Yukon-Tanana and Slide Mountain terranes and affiliated overlap assemblages, Finlayson Lake massive sulphide district, southeastern Yukon, *in* Colpron, M. and Nelson, J.L., eds., Paleozoic Evolution and Metallogeny of Pericratonic Terranes at the Ancient Pacific Margin of North America, Canadian and Alaskan Cordillera: Geological Association of Canada, Special Paper 45, p. 75–105.

Murphy, D.C., Mortensen, J.K. and van Staal, C.R., 2009, 'Windy-McKinley' terrane, western Yukon: new data bearing on its composition, age, correlation and paleotectonic settings, *in*, Weston, L.H., Blackburn, L.R. and Lewis, L.L., eds., Yukon Exploration and Geology: Yukon Geological Survey, p. 195–209.

Naibert, T.J., Benowitz, J.A., Wypych, Alicja, Sicard, K.R., and Twelker, Evan, 2018, $^{40}Ar/^{39}Ar$ data from the Tanacross D-1 and D-2, Big Delta B-4 and B-5, and Mount Hayes A-6 quadrangles, Alaska: Alaska Division of Geological & Geophysical Surveys Raw Data File 2018-3, 15 p. https://doi.org/10.14509/30112

———2020, $^{40}Ar/^{39}Ar$ data from the Tanacross D-1 and parts of the D-2, C-1, and C-2 quadrangles, Alaska: Alaska Division of Geological & Geophysical Surveys Raw Data File 2020-12, 35 p. https://doi.org/10.14509/30466

Naibert, T.J., Heizler, M.T., Newberry, R.J., Twelker, Evan, and Wypych, Alicja, 2023, $^{40}Ar/^{39}Ar$ geochronology data from the Tanacross and Eagle quandrangles, Alaska: Alaska Division of Geological & Geophysical Surveys Raw Data File 2023-23, 19 p. https://doi.org/10.14509/31085

Nelson, J.L., Colpron, Maurice, Piercey, S.J., Dusel-Bacon, Cynthia, Murphy, D.C., and Roots, C.F., 2006, Paleozoic tectonic and metallogenetic evolution of pericratonic terranes in Yukon, northern British Columbia and eastern Alaska: Paleozoic Evolution and Metallogeny of Pericratonic Terranes at the Ancient Pacific Margin of North America, Canadian and Alaskan Cordillera, *in* Colpron, Maurice and Nelson, J.L., eds., Geological Association of Canada Special Paper 45, p. 323–360.

Newberry, R.J., 2020, The Mount Fairplay igneous complex: Alaska Division of Geological & Geophysical Surveys Preliminary Interpretive Report 2020-1, 32 p. https://doi.org/10.14509/30463

Newberry, R.J., and Twelker, Evan, 2021, Metamorphism of the Ladue River-Mount Fairplay area, *in* Twelker, Evan, ed., Geologic investigation of the Ladue River-Mount Fairplay area, eastern Alaska: Alaska Division of Geological & Geophysical Surveys Report of Investigation 2021-5B, p. 33–39. https://doi.org/10.14509/30736

Nokleberg, W.J., and Aleinikoff, J.N., 1985, Summary of stratigraphy, structure, and metamorphism of Devonian igneous-arc terranes, northeastern Mount Hayes quadrangle, eastern Alaskan Range, *in* Bartsch-Winkler, Susan, ed., The United States Geological Survey in Alaska; accomplishments during 1984: U.S. Geological Survey Circular 967, p. 66–70.

Pavlis, T.L., Sisson, V.B., Foster, H.L., Nokleberg, W.J., and Plafker, George, 1993, Mid-Cretaceous extensional tectonics of the Yukon-Tanana Terrane, Trans-Alaska Crustal Transect (TACT), east-central Alaska: Tectonics, v. 12, p. 103–122.

Piercey, S.J., Nelson, J.L., Colpron, Maurice, Dusel-Bacon, Cynthia, Roots, C.F., Simard, R.-L. 2006, Paleozoic magmatism and crustal recycling along the ancient Pacific margin of North America, northern Cordillera, *in* Colpron, Maurice, Nelson, J.L. eds., Paleozoic evolution and metallogeny of pericratonic terranes at the ancient Pacific margin of North America, Canadian and Alaskan Cordillera: Geological Association of Canada Special Paper 45, p. 281–322.

Richter, D.H., 1975, Geologic map of the Nabesna Quadrangle, Alaska: U.S. Geological Survey Miscellaneous Field Studies Map 655-A, 1 sheet, scale 1:250,000.

Roe, J.T., and Stone, D.B., 1993, Paleomagnetism of the Fairbanks basalts, interior Alaska, *in* Solie, D.N., and Tannian, Fran, eds., Short Notes on Alaskan Geology 1993: Alaska Division of Geological & Geophysical Surveys Professional Report 113G, p. 61–69. https://doi.org/10.14509/2311

Ryan, J.J., Zagorevski, Alexandre, Roots, C.F., and Joyce, N.L., 2014, Paleozoic tectonostratigraphy of the northern Stevenson Ridge area, Yukon: Geological Survey of Canada, Current Research (Online) no. 2014-4, 16 p. https://doi.org/10.4095/293924

Ryan, J.J., Zagorevski, Alexandre, Williams, S.P., Roots, C.F., Ciolkiewicz, Wiltold, Hayward, Nathan, and Chapman, J.B., 2013, Geology, Stevenson Ridge (northwest part), Yukon. Geological Survey of Canada, Canadian Geoscience Map 117 (2nd edition, preliminary), scale 1:100,000. https://doi.org/10.4095/292408

Sanchez, M.G., Allan, M.M., Hart, C.J., and Mortensen, J.K., 2014, Extracting ore-deposit-controlling structures from aeromagnetic, gravimetric, topographic, and regional geologic data in western Yukon and eastern Alaska: Interpretation, v. 2, p. SJ75–SJ102. https://doi.org/10.1190/INT-2014-0104.1

Schmidt, M.W., 1992, Amphibole composition in tonalite as a function of pressure: an experimental calibration of the Al-in-hornblende barometer. Contributions to Mineralogy and Petrology, v. 110, p. 304–310. https://doi.org/10.1007/BF00310745

Schmidt, M.W., and Thompson, A.B., 1996, Epidote in calc-alkaline magmas: An experimental study of stability, phase relationships, and the role of epidote in magmatic evolution. American Mineralogist, v. 81, p. 462–474.

Sicard, K.R., Naibert, T.J., Hubbard, T.D., Twelker, Evan, Wypych, Alicja, Werdon, M.B., Willingham, A.L., Gillis, R.J., Lande, L.L., and Newberry, R.J., 2017, Geologic map of the Tok River area, Tanacross A-5 and A-6 quadrangles, eastern Alaska Range, Alaska: Alaska Division of Geological & Geophysical Surveys Preliminary Interpretive Report 2017-3, 15 p., 1 sheet, scale 1:63,360. https://doi.org/10.14509/29722

Simard, R.L., Dostal, Jaroslav, and Roots, C.F., 2003, Development of late Paleozoic volcanic arcs in the Canadian Cordillera: an example from the Klinkit Group, northern British Columbia and southern Yukon, Canadian Journal of Earth Sciences, v. 40, p. 907–924.

Skipton, Diane, 2022, Updated bedrock geology of the southern Nash Creek area in central Yukon (parts of NTS 106D/2, 3, 6 and 7), *in* MacFarlen, K.E., ed., Yukon Exploration and Geology 2021: Yukon Geological Survey, p. 161–183.

Solie, D.N., Werdon, M.B., Freeman, L.K., Newberry, R.J., Szumigala, D.J., Speeter, G.G., and Elliott B.A., 2019, Bedrock-geologic map, Alaska Highway Corridor, Tetlin Junction, Alaska, to Canada Border: Alaska Division of Geological & Geophysical Surveys Preliminary Interpretative Report 2019-3, 16 p., 2 sheets, scale 1:63,360. doi.org/10.14509/30038

Szumigala, D.J., Werdon, M.B., Newberry, R.J., Athey, J.E., Clautice, K.H., Flynn, R.L., Grady, J.C., Munly, W.C., and Johnson, M.R., 2002a, Major-oxide, minor-oxide, trace-element, rare-earth element, trace geochemical, and coal quality data from rocks collected in the Eagle and Tanacross quadrangles, Alaska in 1999, 2000, 2001: Alaska Division of Geological & Geophysical Surveys Raw Data File 2002-1, 35 p., 1 sheet, scale 1:63,360. https://doi.org/10.14509/2866

Szumigala, D.J., Newberry, R.J., Werdon, M.B., Athey, J.E., Flynn, R.L., and Clautice, K.H., 2002b, Bedrock geologic map of the Eagle A-1 Quadrangle, Fortymile mining district: Alaska Division of Geological & Geophysical Surveys Preliminary Interpretive Report 2002-1B, 1 sheet, scale 1:63,360. https://doi.org/10.14509/2864

Todd, Erin, Kylander-Clark, Andrew, Kreiner, D. C., Jones, J. V., III , Holm-Denoma, C. S. and Wypych, Alicja, 2023, U-Pb ages, Hafnium isotope ratios, and trace element concentrations by Laser-ablation Split Stream (LASS) Analysis of igneous and metamorphic zircons from the Yukon-Tanana Upland, eastern Alaska: U.S. Geological Survey Data Release. https://doi.org/10.5066/P9O1DMIE

Todd, Erin, Wypych, Alicja, and Kylander-Clark, Andrew, 2019, U-Pb and Lu-Hf isotope, age, and trace element data from zircon separates from the Tanacross D-1, and parts of D-2, C-1, and C-2 quadrangles: Alaska Division of Geological & Geophysical Surveys Raw Data File 2019-5, 10 p. https://doi.org/10.14509/30198

Twelker, Evan, and O'Sullivan, P.B., 2021, U-Pb detrital zircon geochronology of Cretaceous-Cenozoic sedimentary rocks in the Ladue River-Mount Fairplay area, Alaska: Alaska Division of Geological & Geophysical Surveys Preliminary Interpretive Report 2021-2, 16 p. https://doi.org/10.14509/30683

Twelker, Evan, Newberry, R.J., Wypych, Alicja, Naibert, T.J., Wildland, A.D., Sicard, K.R., Regan, S.P., Athey, J.E., Wyatt, W.C., and Lopez, J.A., 2021, Bedrock geologic map of the Ladue River-Mount Fairplay area, Tanacross and Nabesna quadrangles, Alaska, *in* Twelker, Evan, ed., Geologic investigation of the Ladue River-Mount Fairplay area, eastern Alaska: Alaska Division of Geological & Geophysical Surveys Report of Investigation 2021-5A, p. 1–32, 1 sheet, scale 1:100,000. https://doi.org/10.14509/30735

Weber, F.R., and Wilson, F.H., 2012, Map showing extent of glaciation in the Eagle quadrangle, east-central Alaska: U.S. Geological Survey Open-File Report 2012-1138, 1 sheet, scale 1:2,500,000.

Werdon, M.B., Solie, D.N., Andrew, J.E., Freeman, L.K., Newberry, R.J., Szumigala, D.J., and Elliott, B.A., 2019, Bedrock-geologic map, Alaska Highway corridor, Dot Lake to Tetlin Junction, Alaska: Alaska Division of Geological & Geophysical Surveys Preliminary Interpretive Report 2019-2, 14 p., 2 sheets, scale 1:63,360. https://doi.org/10.14509/30037

Werdon, M.B., Newberry, R.J., and Szumigala, D.J., 2001, Bedrock geologic map of the Eagle A-2 Quadrangle, Fortymile mining district, Alaska: Alaska Division of Geological & Geophysical Surveys Preliminary Interpretive Report 2001-3B, 1 sheet, scale 1:63,360. https://doi. org/10.14509/2670

Wildland, A.D., 2022, Temporal links between ductile shearing, widespread plutonism, and tectonic exhumation near the boundary of parautochthonous and allochthonous terranes in the northern Cordillera, Alaska: Fairbanks, Alaska, University of Alaska Fairbanks, M.S. thesis, 67 p.

Wildland, A.D., Wypych, Alicja, Regan, S.P., and Holland, Mark, 2021, U-Pb zircon ages from bedrock samples collected in the Tanacross and Nabesna quadrangles, eastern Alaska: Alaska Division of Geological & Geophysical Surveys Preliminary Interpretive Report 2021-4, 47 p. https://doi.org/10.14509/30732

Wypych, Alicja, 2021, Geochemistry of the igneous rocks in the Ladue River-Mount Fairplay area, *in* Twelker, Evan, ed., Geologic investigation of the Ladue River-Mount Fairplay area, eastern Alaska: Alaska Division of Geological & Geophysical Surveys Report of Investigation 2021-5E, p. 63–76. https://doi.org/10.14509/30739

Wypych, Alicja, Gavel, M.M., Naibert, T.J., Avirett, D.F., Barrera, M.L., Hubbard, A.K., Newberry, R.J., Regan, S.P., Twelker, Evan, Wildland, A.D., and Wyatt, W.C., 2022a, Geochemical data from samples collected in 2020 and 2021 for the Western Tanacross project, Tanacross Quadrangle, Alaska: Alaska Division of Geological & Geophysical Surveys Raw Data File 2022-5, 3 p. https://doi.org/10.14509/30844

Wypych, Alicja, Gavel, M.M., Naibert, T.J., Avirett, D.F., Barrera, M.L., Hubbard, A.K., Newberry, R.J., Regan, S.P., Twelker, Evan, Wildland, A.D., and Wyatt, W.C., 2022b, Geochemical data from samples collected in 2021 for the Taylor Mountain project, Tanacross and Eagle quadrangles, Alaska: Alaska Division of Geological & Geophysical Surveys Raw Data File 2022-4, 3 p. https://doi.org/10.14509/30843

Wypych, Alicja, Hubbard, T.D., Naibert, T.J., Athey, J.E., Newberry, R.J., Sicard, K.R., Twelker, Evan, Werdon, M.B., Willingham, A.L., Wyatt, W.C., and Lockett, A.C., 2021, Northeast Tanacross geologic map and map units and descriptions, *in* Wypych, Alicja, ed., Northeast Tanacross geologic mapping project, Alaska: Alaska Division of Geological & Geophysical Surveys Report of Investigation 2020-9B, p. 9–26, 1 sheet, scale 1:63,360. https://doi.org/10.14509/30539

Wypych, Alicja, Jones, J.V., III, and O'Sullivan, Paul, 2020, U-Pb Zircon ages from bedrock samples collected in the Tanacross D-1, and parts of the D-2, C-1, and C-2 quadrangles, Alaska: Alaska Division of Geological & Geophysical Surveys Preliminary Interpretive Report 2020-2, 19 p. https://doi.org/10.14509/30465

Yukon Geological Survey, 2019, Yukon Digital Bedrock Geology. https://yukon.ca/en/yukon-geology#bedrock-geology [accessed: 3/19/2019]

Yukon Geological Survey, 2020, Yukon Geochronology–A database of Yukon isotopic age determinations: Yukon Geological Survey. http://data.geology.gov.yk.ca/Compilation/22 [accessed February 1, 2021]